

University of Windsor

## Scholarship at UWindor

---

Electronic Theses and Dissertations

Theses, Dissertations, and Major Papers

---

3-10-2019

### A Hybrid Indoor Location Positioning System

Shuo Li

*University of Windsor*

Follow this and additional works at: <https://scholar.uwindsor.ca/etd>

---

#### Recommended Citation

Li, Shuo, "A Hybrid Indoor Location Positioning System" (2019). *Electronic Theses and Dissertations*. 7643.

<https://scholar.uwindsor.ca/etd/7643>

This online database contains the full-text of PhD dissertations and Masters' theses of University of Windsor students from 1954 forward. These documents are made available for personal study and research purposes only, in accordance with the Canadian Copyright Act and the Creative Commons license—CC BY-NC-ND (Attribution, Non-Commercial, No Derivative Works). Under this license, works must always be attributed to the copyright holder (original author), cannot be used for any commercial purposes, and may not be altered. Any other use would require the permission of the copyright holder. Students may inquire about withdrawing their dissertation and/or thesis from this database. For additional inquiries, please contact the repository administrator via email ([scholarship@uwindsor.ca](mailto:scholarship@uwindsor.ca)) or by telephone at 519-253-3000ext. 3208.

# **A Hybrid Indoor Location Positioning System**

By

**Shuo Li**

A Thesis

Submitted to the Faculty of Graduate Studies  
through the Department of Electrical and Computer Engineering  
in Partial Fulfillment of the Requirements for  
the Degree of Master of Applied Science  
at the University of Windsor

Windsor, Ontario, Canada

© 2019 Shuo Li

**A Hybrid Indoor Location Positioning System**

by

**Shuo Li**

APPROVED BY:

---

G. Reader

Department of Mechanical, Automotive and Materials Engineering

---

S. Erfani

Department of Electrical and Computer Engineering

---

R. Muscedere, Co-Advisor

Department of Electrical and Computer Engineering

---

R. Rashidzadeh, Co-Advisor

Department of Electrical and Computer Engineering

January 9, 2019

## DECLARATION OF CO-AUTHORSHIP/PREVIOUS PUBLICATIONS

### I. Co-Authorship

I hereby declare that this thesis incorporates materials that are the results of joint research, as follows: Chapter 3 of the thesis was co-authored with Dr. Rashid Rashidzadeh. Chapter 4 of the thesis was co-authored with Dr. Rashid Rashidzadeh and Dr. Roberto Muscedere. In all cases, the key ideas, primary contributions, experimental designs, data analysis, interpretation, and writing were performed by the author. Dr. Rashid Rashidzadeh contributed to the statistical analysis and graphing results; Dr. Roberto Muscedere provided feedback on refinement of ideas and editing manuscript.

I am aware of the University of Windsor Senate Policy on Authorship and I certify that I have properly acknowledged the contribution of other researchers to my thesis and have obtained written permission from the co-author to include the materials in my thesis.

I certify that, with the above qualification, this thesis, and the research to which it refers, is the product of my own work.

### II. Previous Publications

This thesis includes 2 original articles that have been previously published/submitted for publication in peer reviewed journals, as follows:

<b>Chapter</b>	<b>Publication Title</b>	<b>Publication Status</b>
<b>Chapter -3</b>	S.Li, R. Rashidzadeh, "A Hybrid Indoor Location Positioning System," 2018 IEEE International Conference on Electro/Information Technology (EIT), Rochester, MI, 2018, pp. 0187-0191.	Published
<b>Chapter -4</b>	S.Li, R. Rashidzadeh and R. Muscedere, "An Indoor Location Estimation System with Fine and	Submitted for review

	Coarse Positioning Modes," IET Wireless Sensor Systems.	
--	--	--

I certify that I have obtained a written permission from the copyright owner(s) to include the above published material(s) in my thesis. I certify that the above material describes work completed during my registration as a graduate student at the University of Windsor.

### III. General

I declare that, to the best of my knowledge, my thesis does not infringe upon anyone's copyright nor violate any proprietary rights and that any ideas, techniques, quotations, or any other material from the work of other people included in my thesis, published or otherwise, are fully acknowledged in accordance with the standard referencing practices. Furthermore, to the extent that I have included copyrighted material that surpasses the bounds of fair dealing within the meaning of the Canada Copyright Act, I certify that I have obtained a written permission from the copyright owners to include such materials in my thesis.

I declare that this is a true copy of my thesis, including any final revisions, as approved by my thesis committee and the Graduate Studies office, and that this thesis has not been submitted for a higher degree to any other University or Institution.

## ABSTRACT

Indoor location positioning techniques have experienced impressive growth in recent years. A wide range of indoor positioning algorithms has been developed for various applications. In this work a practical indoor location positioning technique is presented which utilizes off-the-shelf smartphones and low-cost Bluetooth Low Energy (BLE) nodes without any further infrastructure. The method includes coarse and fine modes of location positioning. In the coarse mode, the received signal strength (RSS) of the BLE nodes is used for location estimation while in the fine acoustic signals are utilized for accurate positioning. The system can achieve centimeter-level positioning accuracy in its fine mode. To enhance the system's performance in noisy environments, two digital signal processing (DSP) algorithms of (a) band-pass filtering with audio pattern recognition and (b) linear frequency modulated chirp signal with matched filter are implemented. To increase the system's robustness in dense multipath environments, a method using data clustering with sliding window is employed. The received signal strength of BLE nodes is used as an auxiliary positioning method to identify the non-line-of-sight (NLoS) propagation paths in the acoustic positioning mode. Experimental measurement results in an indoor area of 10 m<sup>2</sup> indicate that the positioning error falls below 6 cm.

## DEDICATION

*I dedicate this work to my parents*

## ACKNOWLEDGEMENTS

I would like to thank my supervisor Dr. Rashid Rashidzadeh for his guidance, encouragement and support to complete my research studies. I am grateful for his involvement, mentoring and his constructive technical advice.

I am grateful to my co-supervisor Dr. Roberto Muscedere for his valuable comments and technical support which help me to improve my work and overcome technical challenges.

I would also like to thank my committee members Dr. S. Erfani and Dr. G. Reader for their constructive comments and positive criticism.

I would like to extend my gratitude to my colleagues at the Research Centre for Integrated Microsystems (RCIM). I appreciate their friendship, support, encouragement, their constant involvement and valuable feedback.

Finally, I would like to thank the research and financial support received from Natural Sciences and Engineering Research Council (NSERC) of Canada and Canadian Microelectronics Corporation (CMC) Microsystems.

TABLE OF CONTENTS

DECLARATION OF CO-AUTHORSHIP/PREVIOUS PUBLICATIONS .....iii

ABSTRACT..... v

DEDICATION..... vi

ACKNOWLEDGEMENTS .....vii

LIST OF TABLES ..... xi

LIST OF FIGURES .....xii

LIST OF ABBREVIATIONS.....xiv

Chapter -1..... 1

**Introduction..... 1**

**1.1 Indoor Location Based Applications and Accuracies ..... 1**

**1.2 Dual Mode Positioning ..... 1**

**1.3 System Cost and Smartphone Compatibility .....2**

**1.4 Problem Statement: Lack of a Practical Indoor Positioning System .....2**

**1.5 Research Goals.....3**

**1.6 Thesis Overview .....3**

**1.7 References.....4**

Chapter -2..... 5

**Related Work .....5**

**2.1 RF Signal .....5**

**2.2 Audio Signal .....5**

**2.3 Light Signal and Magnetic Field.....6**

**2.4 Strengths and Weakness of the Proposed Solutions .....6**

**2.5 References..... 7**

Chapter -3..... 8

**A Hybrid Indoor Location Positioning System .....8**

**3.1 Introduction.....8**

**3.2 General Positioning Method .....9**

**3.2.1 Dual Mode Positioning.....9**

**3.2.2 System Architecture.....9**

3.3	<b>Fine Positioning Approach</b> .....	11
3.3.1	<b>Multilateration Positioning</b> .....	11
3.3.2	<b>TDoA Measurement</b> .....	12
3.3.3	<b>Audio Signal Arrival Detection</b> .....	14
3.4	<b>Experimental Validation</b> .....	17
3.4.1	<b>System Prototype</b> .....	17
3.4.2	<b>Experiment Setup</b> .....	18
3.4.3	<b>Experiment Result</b> .....	19
3.5	<b>Conclusion</b> .....	19
3.6	<b>References</b> .....	19
Chapter -4.....		21
<b>An Indoor Location Estimation System with Fine and Coarse Positioning Modes</b>		21
4.1	<b>Introduction</b> .....	21
4.2	<b>Related Work</b> .....	22
4.3	<b>System Overview</b> .....	23
4.3.1	<b>Dual Mode Positioning</b> .....	23
4.3.2	<b>Multilateration Positioning</b> .....	23
4.4	<b>ToA Estimation</b> .....	27
4.4.1	<b>Linear Frequency Modulated Chirp &amp; Matched Filtering</b> .....	27
4.4.2	<b>Indoor Acoustic Environment Modeling</b> .....	29
4.4.3	<b>Noise Filtering</b> .....	31
4.4.4	<b>ToA Point Selection</b> .....	33
4.4.5	<b>NLoS Identification</b> .....	37
4.5	<b>Experimental Validation</b> .....	40
4.5.1	<b>System Prototype</b> .....	40
4.5.2	<b>Wireless Communication</b> .....	41
4.5.3	<b>Optimal Node Placement</b> .....	41
4.5.4	<b>Experiment Setup</b> .....	42
4.5.5	<b>Experiments Results</b> .....	46
4.6	<b>Conclusion</b> .....	46
4.7	<b>References</b> .....	46
Chapter -5.....		50

<b>Conclusions and future work</b> .....	50
<b>5.1 Conclusions</b> .....	50
<b>5.2 Future Work</b> .....	51
<b>APPENDIX : COPY RIGHT PERMISSION</b> .....	52
<b>VITA AUCTORIS</b> .....	53

## LIST OF TABLES

<b>Table #</b>	<b>Caption</b>	<b>Page #</b>
<b>1</b>	Comparison of Different Systems	7
<b>2</b>	Noise Correlation Coefficients Tests	33

## LIST OF FIGURES

<b>Figure #</b>	<b>Caption</b>	<b>Page #</b>
<b>1</b>	An indoor environment divided to 3 grids	11
<b>2</b>	Smartphone and audio receivers' coordinates	11
<b>3</b>	Audio signals received at 2 audio receivers	14
<b>4</b>	Audio signal emitted from smartphone	14
<b>5</b>	Noise near 17 KHz	15
<b>6</b>	Sensortag used as an audio receiver	17
<b>7</b>	Screenshot of the developed app	17
<b>8</b>	Experiment setup	18
<b>9</b>	Experiment results in quiet environment	19
<b>10</b>	Experiment results in noisy environment	19
<b>11</b>	An indoor environment covered with the system	25
<b>12</b>	Time-of-Arrivals (ToAs) for two nodes and the corresponding Time Difference of Arrival (TDoA)	25
<b>13</b>	Smartphone and audio receivers	26
<b>14</b>	Received chirp signal transferred through a propagation channel with non-flat frequency response	30
<b>15</b>	ToA peak and highest peak	31
<b>16</b>	The calculated threshold for the propagation channel to filter out the noise	33
<b>17</b>	Positive part of $c[n]$ with $N_{ToA} = 6615$ , $F_s = 44.1$ KHz	36
<b>18</b>	Valid cluster and noise	36

<b>19</b>	Separated audio data clusters	37
<b>20</b>	First local maxima as ToA	37
<b>21</b>	Local maxima indicating the ToA point	38
<b>22</b>	LoS condition	39
<b>23</b>	NLoS condition	39
<b>24</b>	The output of the cross correlation for an experiment where (a) with a line-of-sight connection and (b) without a line-of-sight connection between transmitters and receivers	40
<b>25</b>	Wireless communication	41
<b>26</b>	TDoA error tolerance ability with respect to z coordinates	43
<b>27</b>	The area where the experimental measurements were performed	44
<b>28</b>	TDoA experiment results in quiet environment	45
<b>29</b>	TDoA experiment results in noisy environment	45
<b>30</b>	TDoA results under dense multipath effects	46
<b>31</b>	Position estimation results	46

## LIST OF ABBREVIATIONS

RSS	Received Signal Strength Indication
RF	Radio Frequency
GPS	Global Positioning System
BLE	Bluetooth Low Energy
SNR	Signal-to-noise Ratio
TDoA	Time-Difference-of-Arrival
UWB	Ultra-wideband
RFID	Radio Frequency Identification
WLAN	Wireless LAN
ToA	Time-of-Arrival
PDA	Personal Digital Assistant
IoT	Internet of Things
LoS	Line-of-sight
NLoS	Non-line-of-sight
AoA	Angle-of-Arrival
CDMA	Code-division Multiple Access
ToF	Time-of-flight
LFM	Linear Frequency Modulated

## **Chapter -1**

### **Introduction**

The need for an indoor location positioning system has risen dramatically in recent years. The global indoor positioning market is expected to grow at an annual rate of 58.9% from 2017 to 2021 [1]. Indoor location positioning techniques can improve the services provided by health care centers, smart homes, indoor parking lots, museums and shopping malls.

The design of a cost-effective and accurate indoor positioning is a challenging task. The existing global positioning system (GPS), which is a mature positioning solution, doesn't work properly in indoor locations. A GPS based positioning system requires a line of sight connection between transmitters and receivers to ensure positioning accuracy. A practical indoor positioning solution is expected to be cost-effective, easy to use and accurate [2].

#### **1.1 Indoor Location Based Applications and Accuracies**

In general, the accuracy required for indoor positioning is higher than the accuracy required for outdoor navigation. GPS can achieve less than 7.8 meters error in 95% of cases which is good enough for many outdoor positioning applications [3], however, for an indoor area, such an error is not acceptable for most applications.

In a typical application scenario such as a shopping mall, a meter level positioning accuracy [4] is enough to find the desired locations and shops. However, inside a shop, a centimeter level accuracy may be needed to find an item in a department such as a pair of shoes. As presented in this typical application, initially a coarse localization system meets the positioning requirements and then a fine positioning system is needed to locate desired items. In general, a high positioning accuracy increases the costs and power consumption. Using a hybrid system with coarse and fine positioning capacity reduces the costs.

#### **1.2 Dual Mode Positioning**

The proposed system in this work can switch between a meter-level coarse mode positioning and a centimeter-level fine positioning mode. The coarse positioning mode is based on the Received Signal Strength (RSS) method while the fine positioning mode utilizes an acoustic signal for accurate positioning.

- i. **Fine positioning mode:** In the fine mode the system utilizes sound pulses transmitted from a smartphone to perform the positioning. A smartphone can generate sound with the maximum frequency of about 20 KHz [5]. BLE tags with the capacity to detect the transmitted audio signals are placed at known locations in the environment. The BLE tags calculate the Time of Arrival (ToA) for the received audio signals and send this information back to the smartphone to determine its location.
- ii. **Power consumption:** The DSP algorithms for the fine mode are computationally costly. To decrease the power consumption, the micro-controller is set to operate in the sleep mode. It is only activated when a high accuracy positioning is required.
- iii. **Coarse positioning mode:** Though the audio-based positioning method can achieve a centimeter level accuracy, it consumes a considerable amount of power. The systems by default operate in the RSS based positioning mode [6] which consumes less power and switches to the fine-positioning mode when it is needed. Moreover, the BLE RSS positioning mode is used as a reference to detect outliers in the fine-positioning mode.

### **1.3 System Cost and Smartphone Compatibility**

The system's cost includes the costs of the resources needed for deployment and maintenance. The deployment costs mainly cover the costs of hardware, such as the tags and the costs of roaming devices. To lower the costs, the total number of tags have to be optimized, which means that the coverage area for each beacon should be as large as possible. After installation, the cost mainly comes from the battery replacement and software updates.

Considering the ubiquity of smartphones, a system requiring nothing but a smartphone at the user side appeals more to customers compared to a system requiring custom designed devices.

### **1.4 Problem Statement: Lack of a Practical Indoor Positioning System**

In general, for indoor people location tracking and positioning, a system should be accurate, low cost and smartphone compatible.

There are many RSS-based indoor positioning systems proposed in the literature, they can achieve meter-level accuracy, however, many indoor applications require centimeter level accuracies. There are also some high accuracy indoor positioning systems, but they are relatively costly. Some ultrasound solutions can achieve both high accuracy and low cost, but they are not smartphone compatible.

### **1.5 Research Goals**

The main purpose of this work is to develop an indoor positioning solution that can be implemented for real-world applications. The main contributions of this thesis are:

- i. A new hybrid indoor positioning system with coarse and fine positioning modes is designed, implemented and tested. The implemented system is cost-effective and supports cellphone platforms.
- ii. A new DSP algorithm is developed to increase the range and to overcome the environmental noise and multipath effects in the fine positioning mode.

### **1.6 Thesis Overview**

This thesis is organized as follows:

Chapter -1 introduces the research topic, provides an overview of the related work and available indoor positioning methods.

Chapter -2 discusses the proposed indoor positioning solutions, compares their strengths and weaknesses.

Chapter-3 presents the hardware implementation and the corresponding positioning algorithms. This work has been published in the 2018 IEEE International Conference on Electro/Information Technology (EIT).

Chapter-4 presents the hybrid positioning solution and the associated DSP algorithms. The results of this work have been submitted to the journal of IET Wireless Sensor Systems for review.

Chapter-5 summarizes the thesis results and includes the conclusion and future work.

## 1.7 References

- [1] I. Market, "Indoor Location Market by Technology & application - Global Forecast 2022 | MarketsandMarkets," Marketsandmarkets.com, 2018. [Online]. Available: <https://www.marketsandmarkets.com/Market-Reports/indoor-positioning-navigation-ipin-market-989.html>. [Accessed: 23- Nov- 2018].
- [2] S. Li, R. Rashidzadeh, "A Hybrid Indoor Location Positioning System," 2018 IEEE International Conference on Electro/Information Technology (EIT), Rochester, MI, 2018, pp. 0187-0191.
- [3] "GPS.gov: GPS Accuracy," Gps.gov, 2018. [Online]. Available: <https://www.gps.gov/systems/gps/performance/accuracy/>. [Accessed: 23- Nov- 2018].
- [4] R. Brena et al., "Evolution of Indoor Positioning Technologies: A Survey, " Journal of Sensors, vol. 2017, Article ID 2630413, 21 pages, 2017. <https://doi.org/10.1155/2017/2630413>.
- [5] F. Höflinger et al., "Acoustic Self-Calibrating System for Indoor Smartphone Tracking (ASSIST)," 2012 International Conference on Indoor Positioning and Indoor Navigation (IPIN), Sydney, NSW, 2012, pp. 1-9.
- [6] F. Zaki, R. Rashidzadeh, "An Indoor Location Positioning Algorithm for Portable Devices and Autonomous Machines," International Conference on Indoor Positioning and Indoor Navigation (IPIN), Alcalá de Henares, Spain, 2016.

## Chapter -2

### Related Work

There are many indoor positioning solutions proposed in the past. They can be mainly classified as follows [1]:

- i. RF signal.
- ii. Audio signal.
- iii. Light.
- iv. Magnetic field and other signals

#### 2.1 RF Signal

The common solutions using RF signals are based on BLE, Wi-Fi, ZigBee, Radio Frequency Identification (RFID) and UWB technologies. The systems using BLE, Wi-Fi and ZigBee technologies are often range-based systems utilizing the Received Signal Strength (RSS). There are commercial solutions such as Apple's BLE iBeacon, Ekahau using wireless LAN (WLAN) fingerprint and Netvox ZigBee. For the systems using UWB, the positioning results come from the Angle-of-Arrival (AoA) or the Time-Difference-of-Arrival (TDoA) of the UWB signals. An example of the commercial UWB system is Ubisense Real-Time Location System [1].

#### 2.2 Audio Signal

The systems using audio signal often determine a positioning using the Time-of-Arrival (ToA) or TDoA of an audio signal. ActiveBat and Cricket are the successful positioning systems using ultrasound. ActiveBat is an active ultrasonic positioning system while the latter one is passive [2-3]. They can both achieve centimeter-level accuracy using ultrasound. However, these system do not support cellphone platforms and they require custom design hardware. There are also systems using audible or near ultrasound to support cellphone platforms. For example, Beep uses audible sound signal transmitted from a Personal Digital Assistant (PDA) [4], ASSIST uses near ultrasound signal transmitted from a smartphone [5]. Smartphones are used as audio receivers in ALPS and Akkurat for indoor positioning [6-7].

### 2.3 Light Signal and Magnetic Field

There are systems using light and magnetic field for indoor location estimation. Infrared technology and visible light are both utilized for positioning. There are also systems that utilize the earth's natural magnetic field without any further infrastructure, a commercial example of this type of system is IndoorAtlas [1].

### 2.4 Strengths and Weakness of the Proposed Solutions

The strengths and weaknesses of the systems proposed in the past are summarized in Table-I using accuracy and smartphone compatibility as criteria for comparison.

TABLE I. COMPARISON OF DIFFERENT SYSTEMS

<i>Signal types</i>	<i>Accuracy</i>	<i>Smartphone Compatibility</i>
BLE	Around 1 m	Yes
Wi-Fi	Around 1 m	Yes
UWB	<10 cm	No
ZigBee	Meters	Yes
RFID	1-5 m	No
Ultrasound	<10 cm	No
Audible/Near ultrasound	<10 cm	Yes
Light	Meters	Some
Magnetic field	Meters	Yes

Form the above table it can be concluded that systems using audio signals support a higher accuracy level while maintaining the smartphone compatibility requirement.

## 2.5 References

- [1] R. Brena et al., "Evolution of Indoor Positioning Technologies: A Survey," *Journal of Sensors*, vol. 2017, Article ID 2630413, 21 pages, 2017. <https://doi.org/10.1155/2017/2630413>.
- [2] N. Priyantha, A. Chakraborty and H. Balakrishnan, "The cricket location-support system," *Proc. ACM Conference on Mobile Computing and Networking*, 2000.
- [3] A. Ward, A. Jones and A. Hopper, "A New Location Technique for the Active Office," *IEEE Personal Communications*, Vol. 4, No. 5, October 1997, pp. 42-47.
- [4] A. Mandal et al., "Beep: 3D indoor positioning using audible sound," *Second IEEE Consumer Communications and Networking Conference, 2005. CCNC. 2005, Las Vegas, NV, 2005*, pp. 348-353.
- [5] F. Höflinger et al., "Acoustic Self-calibrating System for Indoor Smartphone Tracking (ASSIST)," *2012 International Conference on Indoor Positioning and Indoor Navigation (IPIN)*, Sydney, NSW, 2012, pp. 1-9.
- [6] L. Patrick et al., "ALPS: A Bluetooth and Ultrasound Platform for Mapping and Localization," 73-84. [10.1145/2809695.2809727](https://doi.org/10.1145/2809695.2809727).
- [7] S. Lopes et al., "Accurate smartphone indoor positioning using a WSN infrastructure and non-invasive audio for TDoA estimation," *Pervasive and Mobile Computing*, Volume 20, 2015, Pages 29-46. <https://doi.org/10.1016/j.pmcj.2014.09.003>.
- [8] R. Balani, "Energy Consumption Analysis for Bluetooth, WiFi and Cellular Networks," Document, Electrical Engineering, University of California at Los Angeles.

## Chapter -3

### A Hybrid Indoor Location Positioning System

#### 3.1 Introduction

The use of indoor location positioning systems has risen significantly in recent years. They are widely used in areas such as health care centers, smart homes and shopping malls. Location positioning with a high level of accuracy in indoor environments is proven to be challenging [1]. Indoor positioning systems utilizing electromagnetic waves and received signal strengths suffer from multipath effects which reduces the positioning accuracy considerably.

There are many indoor positioning solutions in the literature using various techniques and technologies such as vision, infrared, ultrasound, WLAN/Wi-Fi, RFID and ultrawide-band, to perform accurate positioning. The positioning accuracy for methods utilizing Received Signal Strength (RSS) from WiFi access ports or Bluetooth tags is limited due to the nature of electromagnetic wave propagation in indoor environments. To increase the positioning accuracy to less than a meter in these methods custom designed devices are commonly needed [2]. However, using such devices increases the costs considerably. There is need to a cost-effective and easy to use indoor positioning solution with a high accuracy.

Smartphones have already become a daily necessity for many across the globe, a practical and low cost indoor solution can utilize smartphone resources. The audio system in a typical smartphone can deliver audio signals with frequencies higher than 16 KHz. Such audio signals can be used to implement an acoustic positioning system for indoor environments [3].

In the proposed method in this work, only a smartphone is required at the user side for indoor localization. In the fine positioning mode, short audio wave pulses are transmitted through smartphones. Low cost BLE audio receivers in the environment receive the transmitted signals. Then the positioning system measures the time differences of arrival (TDoA) of the audio signals at different locations to calculate the cellphone position. The audio receivers are synchronized through sub-1 GHz RF signals to ensure a high

positioning accuracy. To improve the system's performance against environment noise, a band pass filter is utilized and a pattern recognition algorithm is developed. The communication between the positioning system and nearby smartphones is performed through BLE tags to reduce the power consumption. The use of BLE tags for localization allows the integration of the proposed positioning system with internet of things (IoT) networks.

The rest of the paper is organized as follows. Section II explains the principal of operation for the proposed localization method and its operation modes. Section III covers the details of the implemented acoustic positioning system. The experimental measurement results are presented in section IV and section V summarizes the results and presents the conclusions.

## **3.2 General Positioning Method**

### **3.2.1 Dual Mode Positioning**

The proposed system combines a coarse positing method using RSS with a fine positioning technique using acoustic signals. A smartphone application is developed to implement the positioning algorithm. As shown in Fig. 1, the indoor area is divided into grids, each grid is covered with BLE tags used as audio receivers. These tags can switch between BLE broadcasting mode and audio sampling mode. By default, the positioning is performed in the coarse mode using the RSS based method. If a more accurate positioning is needed, the user sends a request by the application on the smartphone to switch the mode of nearby BLE tags to the audio sampling mode. Then acoustic signals are used for multilateralization for a centimeter-level positioning accuracy.

### **3.2.2 System Architecture**

The proposed positioning system includes audio receivers and BLE access points. The audio receivers and BLE access points are both BLE tags with different firmware. The acoustic signal is generated by user's smartphone for positioning. As shown in Fig.1, each grid in the diagram is covered by four audio receivers and one BLE access point, the audio receivers with known positions serve as anchor points. These receivers periodically broadcast BLE packet to allow users to perform coarse positioning. For the coarse

positioning in this work, the RSS weighted average is implemented to achieve meter-level positioning accuracy [4].

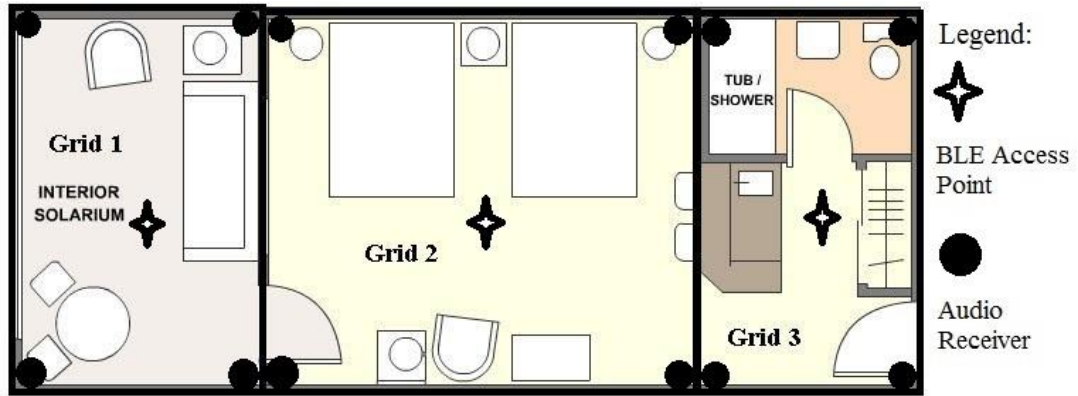


Fig. 1. An indoor environment divided to 3 grids.

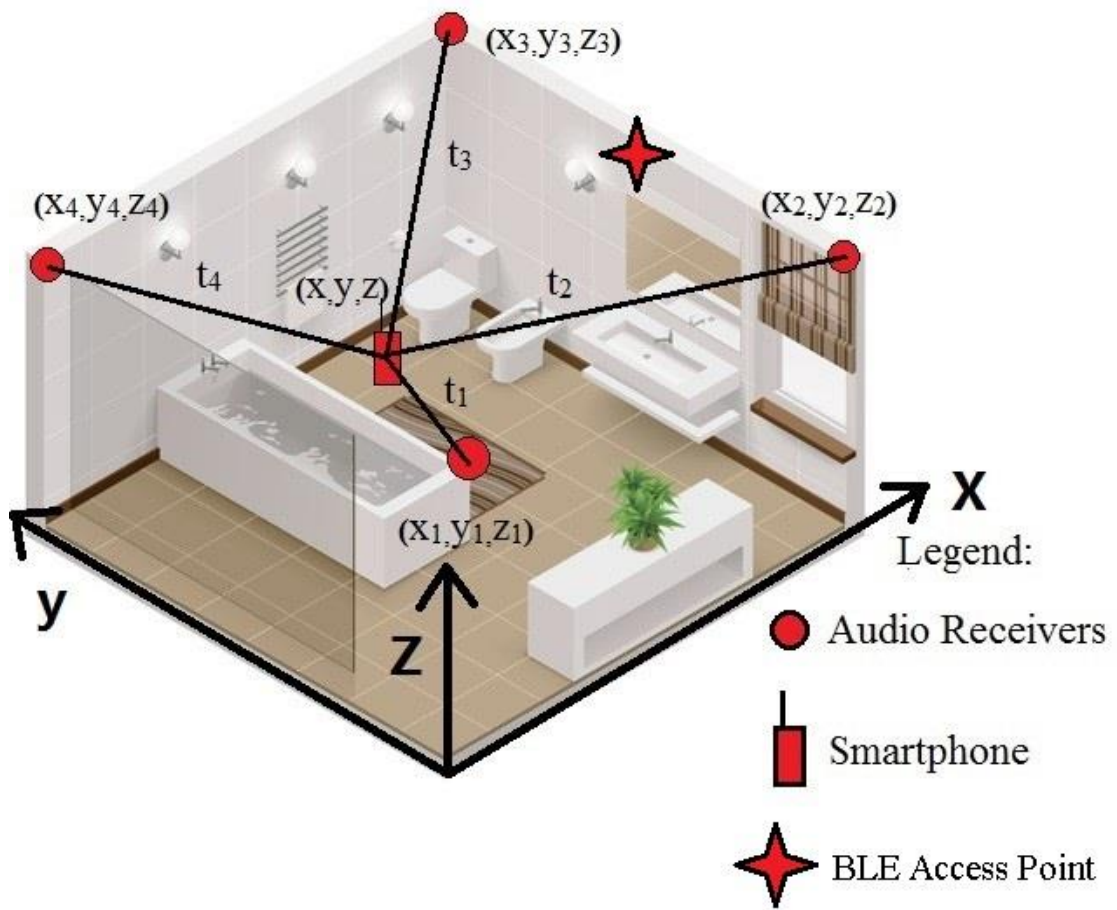


Fig. 2. Smartphone and audio receivers' coordinates.

### 3.3 Fine Positioning Approach

#### 3.3.1 Multilateration Positioning

Smartphone operating systems have audio latency problems that limit their application for accurate time measurement. The elapsed time between a smartphone's audio code execution and the time when the audio is actually played cannot be accurately determined [5]. As a result, in the proposed method in this work instead of the time-of-arrival the Time Difference of Arrival (TDoA) is used for positioning [6]. In the proposed method the distance differences between each audio receiver to the smartphone are required. Fig. 2 illustrates a smartphone and audio receiver's coordinates in a typical indoor environment. Audio receivers serve as anchor points and their  $x$ ,  $y$ ,  $z$  coordinates are known. These coordinates in Fig. 2 can be described as follows.

$$\sqrt{(x-x_2)^2+(y-y_2)^2+(z-z_2)^2}-\sqrt{(x-x_1)^2+(y-y_1)^2+(z-z_1)^2}=v(t_2-t_1) \quad (1)$$

$$\sqrt{(x-x_3)^2+(y-y_3)^2+(z-z_3)^2}-\sqrt{(x-x_1)^2+(y-y_1)^2+(z-z_1)^2}=v(t_3-t_1) \quad (2)$$

$$\sqrt{(x-x_4)^2+(y-y_4)^2+(z-z_4)^2}-\sqrt{(x-x_1)^2+(y-y_1)^2+(z-z_1)^2}=v(t_4-t_1) \quad (3)$$

$v$  indicates the sound speed considered to be 340 m/s, and  $t_1$ - $t_4$  indicate the propagation time from a smartphone to different receivers. It can be seen from the above equations that accurate TDoA measurement is the key for accurate positioning.

We used Chan algorithm [7] to solve the equations. Equation [1]-[3] can be rewritten as:

$$\mathbf{A}\mathbf{X} = \mathbf{B}\mathbf{d}_1 + \mathbf{C} \quad (4)$$

$$\mathbf{A} = \begin{bmatrix} 2(x_2 - x_1) & 2(y_2 - y_1) & 2(z_2 - z_1) \\ 2(x_3 - x_1) & 2(y_3 - y_1) & 2(z_3 - z_1) \\ 2(x_4 - x_1) & 2(y_4 - y_1) & 2(z_4 - z_1) \end{bmatrix}$$

$$\mathbf{X} = \begin{bmatrix} x \\ y \\ z \end{bmatrix} \quad \mathbf{B} = \begin{bmatrix} -2d_{21} \\ -2d_{31} \\ -2d_{41} \end{bmatrix} \quad \mathbf{C} = \begin{bmatrix} r_2^2 - r_1^2 - d_{21}^2 \\ r_3^2 - r_1^2 - d_{31}^2 \\ r_4^2 - r_1^2 - d_{41}^2 \end{bmatrix} \quad (5)$$

where  $d_1 = \sqrt{(x-x_1)^2 + (y-y_1)^2 + (z-z_1)^2}$  and  $r_i^2 = x_i^2 + y_i^2 + z_i^2$ ,  $d_{ij} = v(t_i - t_j)$ .

To make sure that equation [4] can yield the final solution, matrix A has to be invertible which requires a proper placement of the audio receivers. In practice, TDoA measured values have errors, if the errors are too big compared to the grid area,  $d_1$  becomes unsolvable. Simulation results show that increasing the audio receivers' number from 4 to 5 can largely improve both the algorithm's robustness and the positioning accuracy when TDoA values have a relatively large error. In this case for equation [4], the least square method can be used to achieve an optimal solution for x, y, z. However, further increase in the number of audio receivers doesn't have a considerable effect on the robustness and accuracy. In this paper, we used 4 audio receivers in each grid. The above algorithm can achieve a balance between reliability and the computational costs, thus it can be implemented in smartphones.

### 3.3.2 TDoA Measurement

The accuracy of TDoA measurements is of great importance in the proposed indoor positioning system. Fig. 3 shows an audio signal sampled by two audio receivers. The time between the two dash lines in Fig. 3 is the time difference of arrival. The proposed system uses the following algorithm for real-time audio signal processing to measure TDoAs. Once a BLE access point receives the command from a smartphone, it wakes up four adjacent BLE audio receivers. The receivers turn on in the audio sampling mode and all of them sample the incoming acoustic signal simultaneously. The BLE audio receivers process the current sampled block of audio data while sampling the next block. This is to ensure that the audio receivers only detect the first arrival of the audio signals from smartphones which in return eliminates the audio signal multipath effects.

To make sure that the receivers sample the audio data simultaneously. An RF signal is used between audio receivers to achieve an accurate time synchronization. The RF signal runs at 868MHz which will not interference with the BLE communications using 2.4GHz frequency band. The RF core in the sensortags, used as BLE audio receivers, is capable of

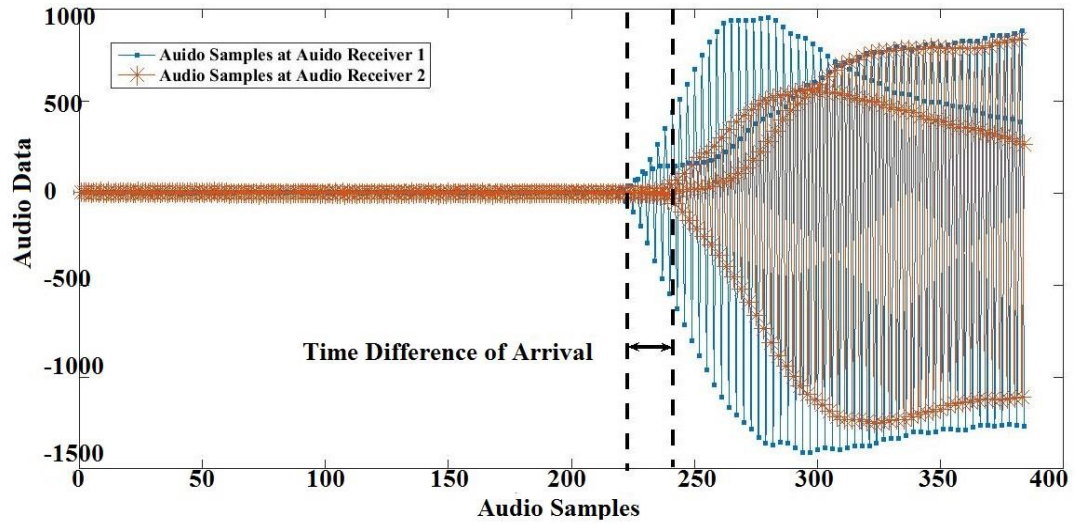


Fig. 3. Audio signals received at 2 audio receivers.

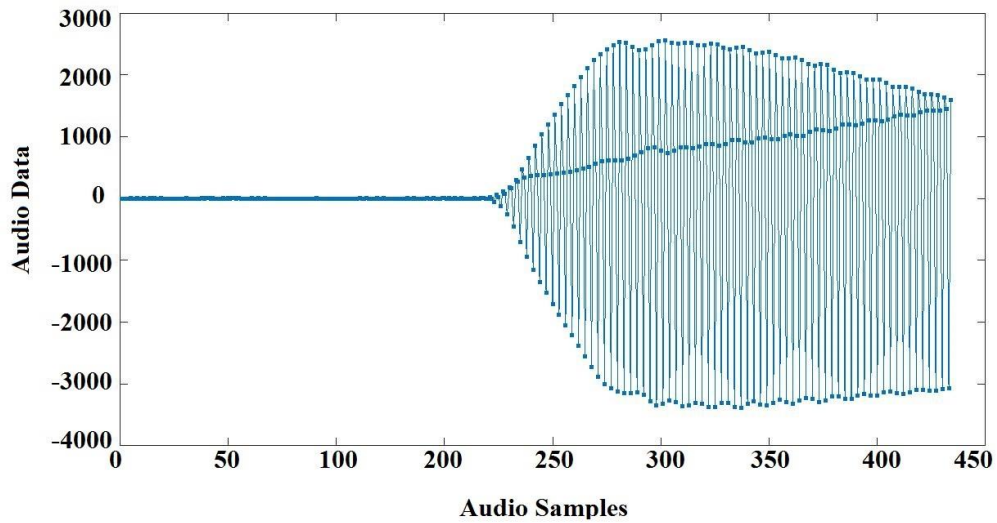


Fig. 4. Audio signal emitted from smartphone.

low power communication and handling RF signals [8].

During the synchronization, the RF transmitter sends a packet containing a time stamp indicating when the RF signal is transmitted, the packet also contains a grid identifier. Initially, the RF receiver looks for incoming RF signal for the purpose of synchronization.

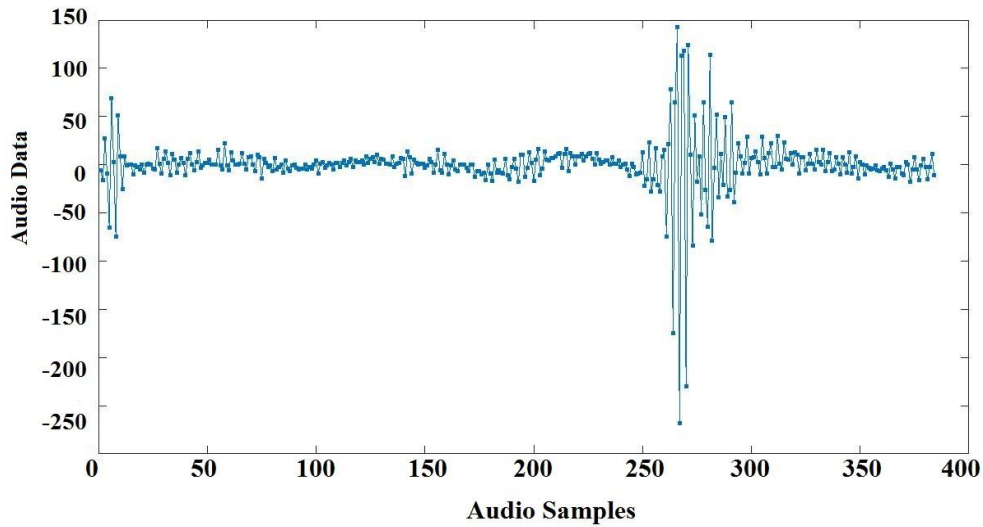


Fig. 5. Noise near 17 KHz.

Once the BLE tags are synchronized, they only communicate at certain point of time, this can save power consumption largely [9].

A relatively high accuracy can be achieved using the above synchronization approach. Experimental results indicate that the time synchronization error is less than  $30.52\mu\text{s}$  which corresponds to the distance measurement error less than 1.04cm.

### 3.3.3 Audio Signal Arrival Detection

An accurate TDoA measurement relies on both accurate time synchronization and proper audio signal arrival detection. However, a proper audio signal arrival detection in a noisy environment is challenging. In the proposed system, a filter at the audio receiver is used to decrease the environment noise. A 2nd-order butterworth band pass filter is designed to limit the noise. Experimental measurement results indicate that the environmental noise is decreased by more than 50dB using the implemented filter. The filter algorithm was optimized to reduce the required processing power from the BLE audio receiver. The optimized filter increases the filtering efficiency by 300%. Experiment results show that prior to the optimization it takes around 16ms to filter one block of audio data while the audio receiver uses about 9ms to sample one block audio data. The optimized filter takes

only about 4ms to process one block of audio data which is shorter than the sampling time of one audio data block, so the optimized filter guarantees the real-time audio processing.

Some indoor events, like metal door slamming can generate high frequency noise entering 17 KHz frequency band and a preset threshold is not enough to filter out all environment noise to detect audio signal's arrival properly in a noisy environment. Moreover, the low-power micro-controller in our system doesn't have enough memory space and processing power to process the entire audio pulse emitted from a smartphone. Therefore, the correlation algorithm to determine the audio signal's time difference of arrival [10] can't be deployed in our system.

To address the problem, a smartphone app is designed in which the audio signal's volume increases continuously once the smartphone starts playing the audio pulse. Moreover, the audio signal's frequency is chosen to be one third of the sampling frequency so the received audio data has 3 distinctly separated branches, i.e. upper, middle and lower branches. Fig. 4 shows the received audio signal's waveform while Fig. 5 indicates the noise signal near 17 KHz, it can be seen that the designed audio pulse has its unique waveform, the difference between upper and lower sides of audio data increases gradually after the starting point, also the difference between either middle and upper or middle and lower sides increases gradually. The audio receivers sample 60 consecutive audio data points after the first audio data point exceeds a preset threshold. Then it checks to see if the received signal's waveform matches the reference signal stored in the memory to distinguish between the desired audio signal and the environmental noise. In a very noisy environment, the desired audio pulse's waveform is degraded by noises at the 17 KHz band. To improve the audio recognition rate in such environments, a moving average filter can be implemented to smooth the received audio waveform. This method will increase the possibility of detecting the transmitted audio signal since its pattern is based on a consecutively changing audio data [11].

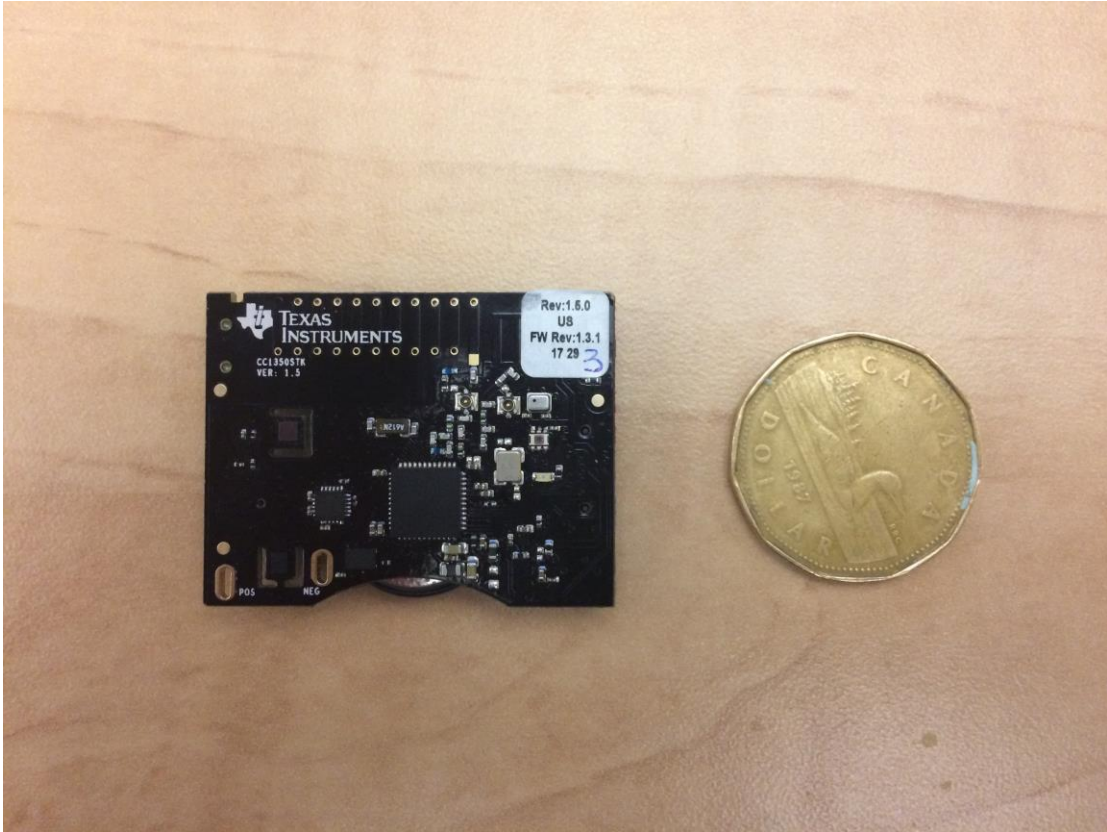


Fig. 6. Sensortag used as an audio receiver.

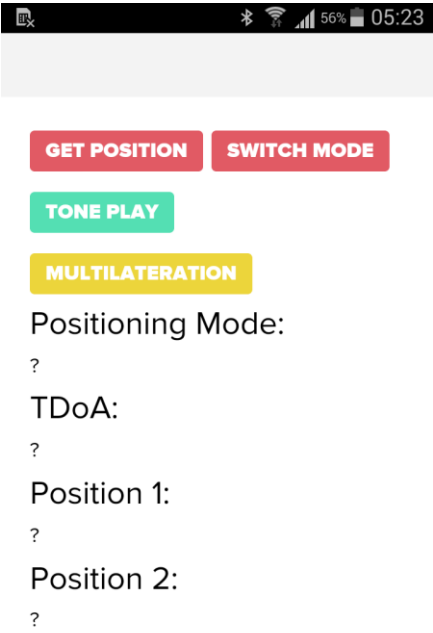


Fig. 7. Screenshot of the developed app.

### 3.4 Experimental Validation

#### 3.4.1 System Prototype

To conduct experimental measurements, a multiplatform application using Apache Cordova framework was developed and installed on an Android based smartphone. CC1350 Sensor tags from Texas Instruments (TI) were used as access points and audio receivers. The sensor tag has a low-power micro-controller and works with a coin battery; however it has powerful radio components which can support dual band wireless communication at 868 MHz and 2.4GHz. Fig. 6 shows a sensor tag used in this work. The firmware of sensor tags were modified to implement the filter and control modules using TI development kit and Code Composer Studio platform.

The developed app can switch between the coarse positioning mode and the fine positioning mode. In the fine positioning mode, the app utilizes smartphone's speaker to send short audio waves. Fig. 7 shows the screenshot of the developed smartphone app.



Fig. 8. Experiment setup.

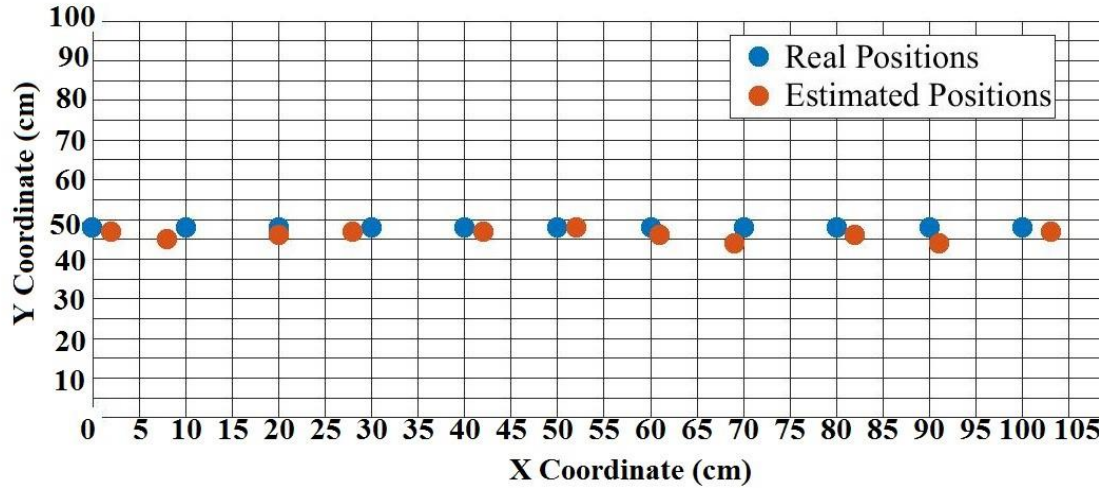


Fig. 9. Experiment results in quiet environment

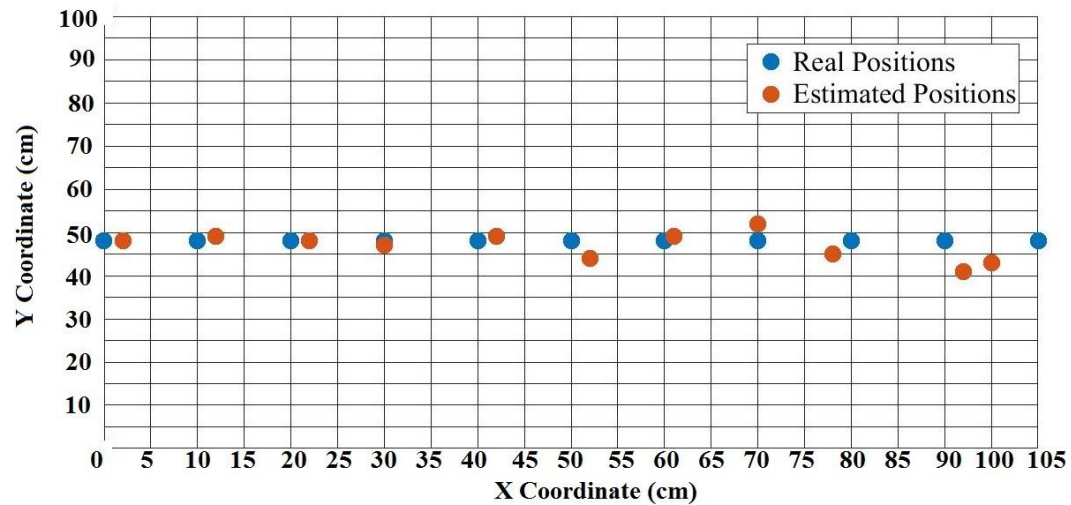


Fig. 10. Experiment results in noisy environment

### 3.4.2 Experiment Setup

As shown in Fig. 8, 4 audio receivers are placed at known locations and a BLE access point is placed at the middle. The experiment was conducted in a quiet environment and a noisy environment. A laptop was placed near the audio receivers playing a recording to simulate the environmental noise during the experiment.

### **3.4.3 Experiment Result**

The experiments were conducted in the second floor of Centre for Engineering Innovation (CEI) building at the University of Windsor for both quiet and noisy environments.

For the quiet environment, users “x” and “y” coordinates were measured with the mean absolute error of 1.64cm and 1.90cm respectively. In a noisy environment, the mean absolute error for “x” and “y” coordinates elevates to 1.81 cm, 2.46 respectively. Fig. 9 shows the results in a quiet environment while Fig. 10 illustrates the results for a noisy environment at different locations. It can be seen that in both noisy and quiet environment the system can achieve centimeter level accuracy. The error for both x and y coordinates falls below 3cm which indicate an overall good positioning accuracy.

### **3.5 Conclusion**

In this work a new indoor positioning systems for smartphones is presented. The proposed system utilizes the received signal strength method for coarse positioning and uses ultrasound for fine positioning. The proposed solution is optimized to reduce the power consumption and the positioning error. Experimental measurement results using Bluetooth Low Energy (BLE) tags indicate that the proposed localization system support a high positioning accuracy in indoor environments with less than 3cm positioning error. The implemented prototype system uses only BLE sensors and a smartphone app for positioning to reduce the implementation costs.

### **3.6 References**

- [1] J. Wendeborg, T. Janson, and C. Schindelbauer, "Self-Localization based on Ambient Signals," *Theoretical Computer Science*, vol.453, pp.98-109, 2012.
- [2] R. Mautz, "Indoor Positioning Technologies, " *Habilitation Thesis*, ETH Zurich, 2012.
- [3] S. Murata et.al., "Accurate Indoor Positioning System using Near-Ultrasonic Sound from a smartphone," *Eighth International Conference on Next Generation*, Oxford, UK, 2014.
- [4] F. Zaki, R. Rashidzadeh, "An Indoor Location Positioning Algorithm for Portable Devices and Autonomous Machines," *International Conference on Indoor Positioning and Indoor Navigation (IPIN)*, Alcalá de Henares, Spain, 2016.

- [5] "Audio Latency | Android NDK | Android Developers", Android Developers, 2017. [Online]. Available: <https://developer.android.com/ndk/guides/audio/audio-latency.html>. [Accessed 29 Sep. 2017].
- [6] S. Lopes et al., "Accurate smartphone indoor positioning using a WSN infrastructure and non-invasive audio for TDoA estimation," *Pervasive and Mobile Computing*, vol. 20, pp. 29-46, 2015.
- [7] Y. Chan, K. Ho, "A simple and efficient estimator for hyperbolic location," *IEEE Transactions on Signal Processing*, vol. 42(8), pp.1905-1915, 1994.
- [8] Texas Instrument, CC1350 SimpleLink™ Ultralow-Power Dual-Band Wireless MCU datasheet (Rev. A). Dallas, TX: 2016.
- [9] "Dev.ti.com. CC13x0 RF User's Guide — CC13x0 Proprietary RF User's Guide 1.01.00 documentation," [online] Available: [http://dev.ti.com/tirex/content/simplelink\\_cc13x0\\_sdk\\_1\\_30\\_00\\_06/docs/proprietary-rf/html/cc13x0/index.html](http://dev.ti.com/tirex/content/simplelink_cc13x0_sdk_1_30_00_06/docs/proprietary-rf/html/cc13x0/index.html) [Accessed 25 Feb. 2018].
- [10]D. Hertz, "Time delay estimation by combining efficient algorithms and generalized cross-correlation methods," *IEEE Transactions on Acoustics, Speech, and Signal Processing*, vol. 34, pp.1-7, 1986.
- [11]"Filtering and Smoothing Data- MATLAB & Simulink", Mathworks.com, 2018. [Online]. Available: <https://www.mathworks.com/help/curvefit/smoothing-data.html>. [Accessed 25 Feb. 2018].

## Chapter -4

### An Indoor Location Estimation System with Fine and Coarse Positioning Modes

#### 4.1 Introduction

Location-aware applications and services are becoming more attractive than ever particularly in indoor environments. GPS is widely used for location positioning however GPS requires a line-of-sight connection between satellite transmitters and a receiver to ensure positioning accuracy. Implementation of a GPS positioning system for indoor areas is costly and unreliable [1]. Many cost-effective solutions have been developed for indoor location estimation in recent years. Indoor positioning systems using received signal strength emerged as low-cost systems achieving acceptable accuracy for many applications [2-3]. Ultra-Wideband (UWB) technology [4] has also appeared for accurate and precision indoor location estimation. However, UWB based systems are relatively costly. Location estimation systems using audio signals support a high-accuracy positioning at low-cost. Due to the widespread use of the cell phones, it is highly desired to design an indoor positioning system that only requires smartphone at the user end.

The proposed system is developed to support off-line cell-phones for location positioning without the need of internet connection. Such a positioning system preserves user privacy as the location information is not shared online. In the proposed solution, Bluetooth Low Energy (BLE) tags with sub-1GHz RF communication are used where the BLE nodes serve as audio receivers. Their power-consumption is lower compared to systems using such nodes as audio transmitters. The BLE nodes RF circuit operate in the sleep mode more than 50% of the time during the operation cycle, they are only activated in certain time points. The Chirp Spread Spectrum (CSS) [2] technique is utilized in the audio mode to increase the range by reducing the effective noise level. Frequency modulated audio waves together with a matched filter are used to support indoor location estimation over a wide range. Moreover, an audio data clustering technique is used to enhance the system's robustness in dense multipath environments. A Non-Line-of-Sight (NLoS) identification method is developed to discard the outliers.

The rest of the paper is organized as follows: Section 3.2 covers the available solutions in the literature, Section 3.3 presents an overview of the proposed system. Section 3.4 explains the details of the implemented DSP algorithms in the acoustic mode. Section 3.5 presents the simulation and the experimental measurement results. Section 3.6 summarizes the results and presents the conclusions.

## **4.2 Related Work**

Acoustic indoor location positioning systems can be classified into two categories of (a) systems using ultrasound and (b) systems using near-ultrasound. Cricket [12] and Active Bat [13] are the two pioneering solutions using ultrasound to localize indoor positions supporting centimeter level accuracy. However, they require custom-designed devices at the user side and they do not support smartphone platforms. Beep [7] uses audible signals with off-the-shelf devices, but its positioning accuracy is low due to the latency at the sound card. Assist [6] utilizes near-ultrasound pulses generated by a smartphone speaker to achieve centimeter level positioning accuracy, however, the use of Wi-Fi NTP protocol for time synchronization increases power-consumption considerably [14]. Akkurate [8] uses smartphones as audio receivers and supports a high positioning accuracy in 2D environments, but the accuracy drops dramatically for a real-world 3D location positioning. The BLE and ultrasound technologies have been used in ALPS [9] for localization in which BLE nodes transmitter acoustic signals. An algorithm is also presented using machine learning techniques to enhance the system's robustness. Murata et al. proposed a high accuracy near-ultrasound positioning system compatible with smartphones; however the positioning accuracy drops considerably in noisy environments [10]. Pérez et al. proposed an android application called LOCATE-US. The system implements code-division multiple access (CDMA) technique to overcome the problems at the acoustic frequency range between 20-22 KHz [11]. Zhang et al. proposed MAIDLOC and RA2LOC systems along with DSP algorithms to enhance the system's performance in noisy and dense multipath locations [15]. They also presented an NLoS identification algorithm using machine learning to discard the outliers due to NLoS propagations [16].

## 4.3 System Overview

### 4.3.1 Dual Mode Positioning

The proposed system combines the RSSI-based positioning algorithm developed by the research team [17] for coarse positioning, and the acoustic positioning method for fine positioning. The RSSI-based positioning method can achieve a meter-level accuracy while the acoustic mode using the Time Difference of Arrival (TDoA) algorithm can achieve centimeter level accuracy. The algorithms are implemented on BLE nodes and supported by a smartphone app. The indoor area, as shown in Fig. 1, is divided into grids. Each grid is covered with the BLE nodes consisting master and slave nodes which can receive audio pulses and broadcast BLE packets. Master nodes directly communicate with the smartphone via BLE. Slave nodes receive inter-node commands from master nodes through sub-1 GHz RF, this architecture consumes less power compared to the method in which each node receives commands directly from the smartphone via BLE. In the coarse positioning mode, BLE packets are transmitted by all BLE nodes and received by smartphones. The user location in this mode is determined using the RSS based algorithm in [17]. In the acoustic mode the smartphone transmits short audio pulses, the BLE nodes receive the pulses and send the results back to the smartphone after applying a DSP algorithm. Acoustic mode positioning is commonly affected by (a) indoor environment audio interferences and (b) lack of line-of-sight propagation. The RSSI-based method is utilized to filter out outliers from acoustic positioning mode as explained in section 3.4.5.

### 4.3.2 Multilateration Positioning

Smartphone operating systems have audio latency problems which leads to inaccurate time-of-flight (ToF) estimation between audio receivers and smartphones. As a result range-based positioning such as trilateration cannot be implemented. A range-free positioning algorithm called multilateration is utilized to overcome the audio latency problem. The difference between the Time-of-Arrivals (ToAs) at the audio receivers are subtracted to get corresponding TDoAs, as shown in Fig. 2. The implemented BLE nodes support sub-1 GHz RF signals used to synchronization all audio receiver nodes [18]. In a room with audio receivers and a smartphone shown in Fig. 3, the user coordinates,  $x$ ,  $y$  and  $z$  can be determined from:

$$\sqrt{(x-x_2)^2+(y-y_2)^2+(z-z_2)^2}-\sqrt{(x-x_1)^2+(y-y_1)^2+(z-z_1)^2}=v(t_2-t_1) \quad (1)$$

$$\sqrt{(x-x_3)^2+(y-y_3)^2+(z-z_3)^2}-\sqrt{(x-x_1)^2+(y-y_1)^2+(z-z_1)^2}=v(t_3-t_1) \quad (2)$$

$$\sqrt{(x-x_4)^2+(y-y_4)^2+(z-z_4)^2}-\sqrt{(x-x_1)^2+(y-y_1)^2+(z-z_1)^2}=v(t_4-t_1) \quad (3)$$

$$\sqrt{(x-x_5)^2+(y-y_5)^2+(z-z_5)^2}-\sqrt{(x-x_1)^2+(y-y_1)^2+(z-z_1)^2}=v(t_5-t_1) \quad (4)$$

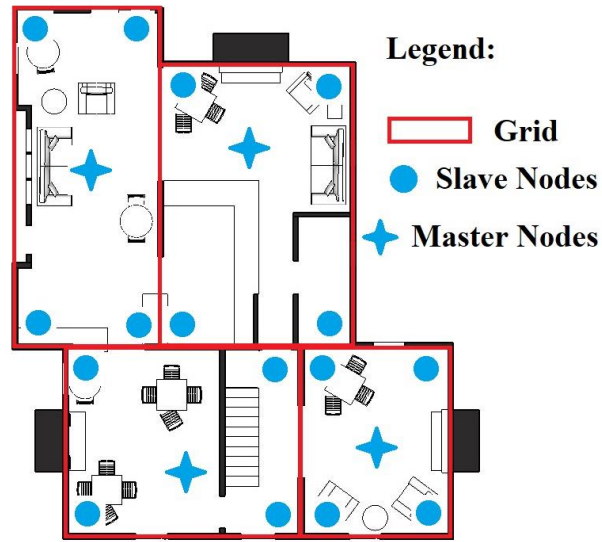


Fig. 1. An indoor environment covered with the system.

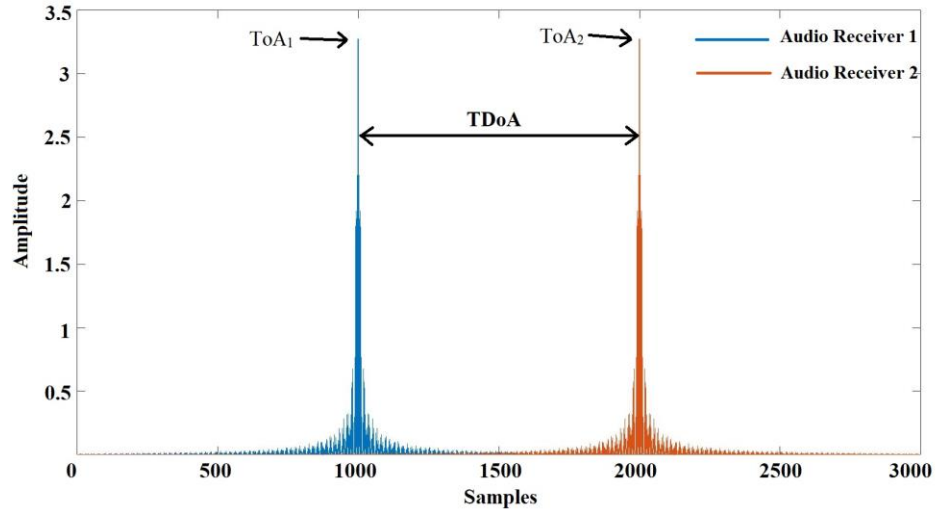


Fig. 2. Time-of-Arrivals (ToAs) for two nodes and the corresponding Time Difference of Arrival (TDoA).

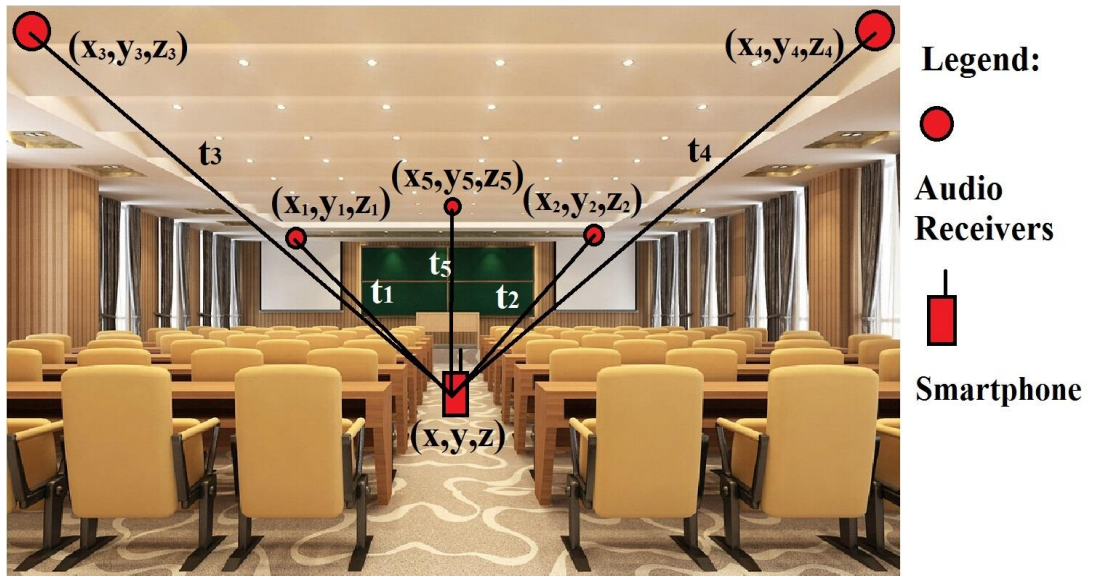


Fig. 3. Smartphone and audio receivers.

Where  $t_1$  to  $t_5$  indicate the time-of-flight to different audio receivers plus the audio latency time. To cancel out the effect of audio latency, the time-difference of arrival is determined. Each ToA is the summation of the time-of-flight and the audio latency time. By pairwise subtracting the ToAs, the effect of unknown latency time is nullified. If we assume the first audio receiver is positioned at the origin, we can use the linear least square algorithm to achieve an optimal solution [19]. We have the following matrixes:

$$\mathbf{A} = \begin{bmatrix} d_{21} & x_2 & y_2 & z_2 \\ d_{31} & x_3 & y_3 & z_3 \\ d_{41} & x_4 & y_4 & z_4 \\ d_{51} & x_5 & y_5 & z_5 \end{bmatrix} \mathbf{b} = \frac{1}{2} \begin{bmatrix} b_2^2 - d_{21}^2 \\ b_3^2 - d_{31}^2 \\ b_4^2 - d_{41}^2 \\ b_5^2 - d_{51}^2 \end{bmatrix}$$

$$\mathbf{y} = \begin{bmatrix} \|\mathbf{X}\| \\ x \\ y \\ z \end{bmatrix} \quad \mathbf{X} = \begin{bmatrix} x \\ y \\ z \end{bmatrix} \quad (5)$$

Where  $d_{ij} = v(t_i - t_j)$ ,  $b_i^2 = x_i^2 + y_i^2 + z_i^2$  and  $\|\mathbf{X}\|$  is the Euclidean vector norm [19]. We then use the linear least squares to achieve the optimal estimation of smartphone coordinate as follows:

$$\tilde{\mathbf{y}} = (\mathbf{A}^T \mathbf{A})^{-1} \mathbf{A}^T \mathbf{b} \quad (6)$$

The above algorithm can provide accurate positioning results. There are also non-linear least square algorithms such as Gauss-Newton, Steepest Descent and Levenberg-Marquardt proposed to further improve the positioning accuracy [17]. These non-linear algorithms first expand equations (1)-(4) at the point  $\mathbf{X}$ , approximate these equations with the 1<sup>st</sup> order Taylor-series, then they use  $\mathbf{X}$  as the initial guess to implement the iterative process to get the final estimated positions. However, these algorithms require the initial point  $\mathbf{X}$  to be close to the real position, otherwise the iterative process may fail to converge [21]. Using the above-mentioned linear least square method, the estimated z coordinates are often far away from their real values. Though the estimation error in the z coordinate will not corrupt the horizontal positioning performance, the above-mentioned algorithms may fail to work. Moreover, an iterative process on a smartphone app may take a long time to converge, so instead of the non-linear least square methods we only utilize linear least square method with an optimal node placement, which will be discussed later. For accurate positioning, the accuracy of ToA estimations are of great importance since TDoAs are

generated by pair-wise subtracting of ToAs. Moreover, an accurate inter-node time synchronization is vital to eliminate the added latency by the nodes.

#### 4.4 ToA Estimation

##### 4.4.1 Linear Frequency Modulated Chirp & Matched Filtering

Linear Frequency Modulated (LFM) Chirp pulse is a sinusoidal wave pulse whose frequency,  $f$ , increases or decreases linearly with time,  $f = f_0 + kt$ . The signal in the time domain can be represented by:

$$x(t) = \cos(2\pi f_0 t + k\pi t^2) \quad (7)$$

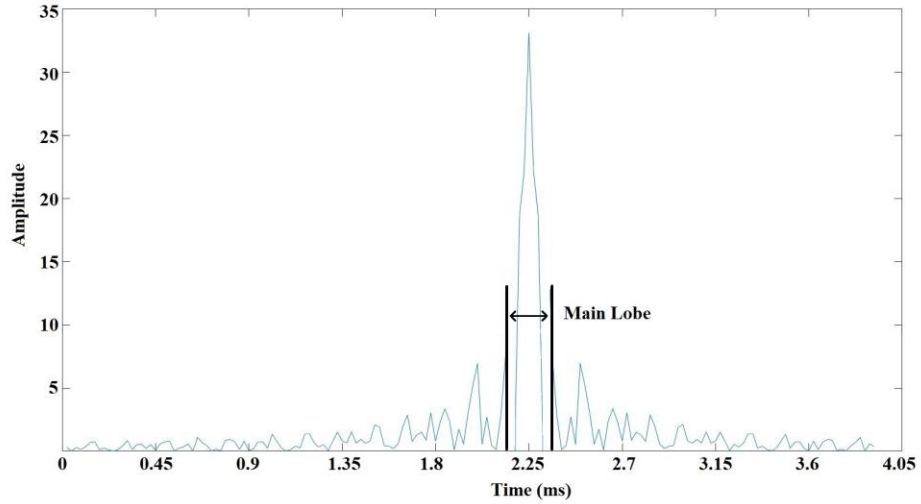


Fig. 4. Cross-correlation function main lobe.

Where  $f_0$  is the initial frequency and  $k$  is the frequency changing rate, in our system the signal's length is 150ms, the initial frequency  $f_0$  is 15kHz and the frequency changing rate  $k$  is 20kHz/s, the transmitted signal is an up-chirp with the bandwidth of 3KHz.

We used a matched filter [22] to determine the chirp's ToA. Ideally, an audio signal,  $x(t)$ , received as:

$$y(t) = \begin{cases} x(t - T_{ToA}) & T_{ToA} \leq t \leq T' \\ 0 & otherwise \end{cases} \quad (8)$$

Where  $T'$  is the chirp's ending time. We cross-correlate the received signal with the reference signal, this is essentially an auto-correlation. The cross-correlation function can be written as:

$$c(\tau) = \int_0^T y(t) \cdot Ref(t - \tau) dt \quad \tau \geq 0 \quad (9)$$

Where  $y(t)$  is the received signal,  $Ref(t)$  is the reference chirp signal and  $T$  is the chirp signal's length. The cross-correlation result can be written as [23]:

$$c(t) = \sqrt{BT} \cdot \text{sinc}[\pi B(t - T_{ToA})] \cdot \cos[2\pi f_0(t - T_{ToA})] \quad (10)$$

Where  $B$  is the chirp signal's bandwidth,  $c(t)$  reaches its peak at  $t = T_{ToA}$  which is the arrival time of the transmitted audio signal.

The energy of the whole received chirp pulse is compressed into the main lobe of  $c(t)$  after the cross-correlation, as shown in Fig. 4. Compared to the original sinc function, its amplitude is increased by the ratio of  $\sqrt{BT}$ , in our system this ratio is about 21. Sound energy attenuates dramatically as the transmission range increases, however with chirp signal and a matched filter, cross-correlation peak corresponding to the ToA point can still be detected even after a propagation range of 20m. Moreover, a chirp signal has a good noise-resistance performance and Doppler effect tolerance. As a result, the combination of a chirp signal and a matched filter is well-suited for ToA estimation of acoustic signals.

In the proposed solution, the algorithm to determine the ToAs runs on the BLE nodes. We compute the cross-correlation in the frequency domain instead of the time domain to reduce the power consumption. The cross-correlation function can be written as:

$$c(t) = IRFFT(Y \cdot REF^*) \quad (11)$$

Where  $IRFFT$  is the inverse real Fourier transform.  $Y$  is the real Fourier transform of the received signal  $y(t)$ , and  $REF$  is the Fourier transform of the reference chirp signal  $Ref(t)$ ,  $REF^*$  is the conjugate of  $REF$ . It takes about 20ms to calculate the cross-correlation for 16384 sample points in the frequency domain, which supports real-time location estimation for many applications.

#### 4.4.2 Indoor Acoustic Environment Modeling

In an ideal case, the received audio signal can be represented by:

$$y(t) = \sum_{i=1}^N a_i x(t - \tau_i) + n(t) \quad (12)$$

Where  $N$  is the number of propagation paths,  $a_i$  indicates different paths' fading coefficients and  $\tau_i$  represents different paths' time delay and  $n(t)$  is white-noise. The signal from the direct propagation path takes the shortest transmission time. The received signal from all paths can be considered as the superposition of replicas of  $x(t)$  with different time delays and energy attenuations. The direct path signal has the strongest energy contribution compared to signals from other paths creating the highest correlation-peak. There is no correlation between the forwarded chirp signal and white noise. Thus the highest correlation-peak is not masked by the audio noise in the environment as long as the noise is not too strong compared to the signal.

In a real-world scenario, the received signals are not the exact replicas of the reference chirp signal  $x(t)$ . The performance parameters of the propagation channels may vary significantly. An acoustic channel's frequency response is ideally considered flat for all in-band frequencies and represented by (13).

$$H(\omega) = \begin{cases} 1 & \omega_1 \leq \omega \leq \omega_2 \\ 0 & \text{otherwise} \end{cases} \quad (13)$$

In a real case, the in-band frequency response is not flat and the received chirp signal may get distorted as indicated in Fig.5. Since the chirp signal's frequency changes linearly with time, the corresponding acoustic channel's frequency response is uneven for all in-band frequencies. The acoustic channel is commonly a smooth curve in the frequency domain. Thus, it can be expressed by a polynomial using Taylor-series. As a result, for every location in a room, no matter how different the acoustic channels are, the frequency responses can be always written as:

$$H(\omega) = \begin{cases} a_n \omega^n + a_{n-1} \omega^{n-1} + \dots + a_0 & \omega_1 \leq \omega \leq \omega_2 \\ 0 & \text{otherwise} \end{cases} \quad (14)$$

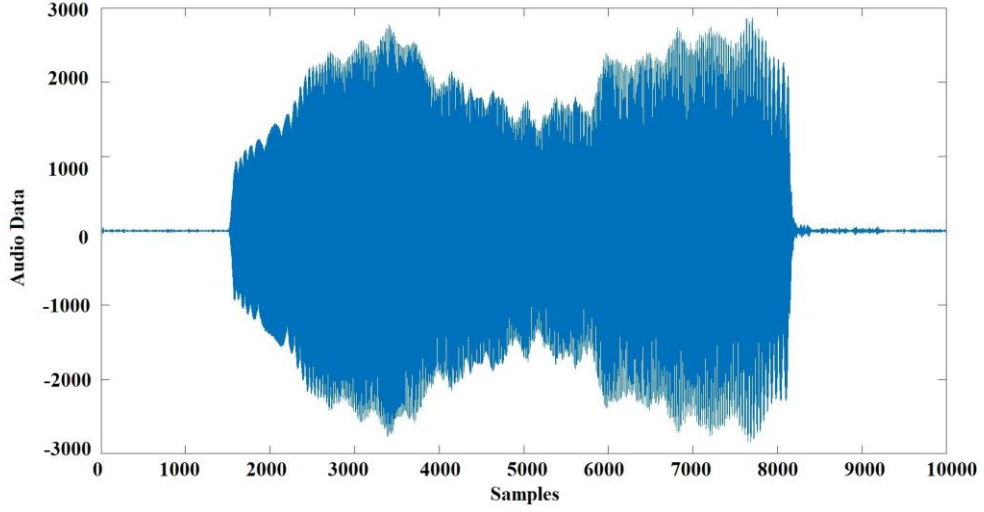


Fig. 5. Received chirp signal transferred through a propagation channel with non-flat frequency response.

As mentioned above, the cross-correlation algorithm can be performed in the frequency domain. Therefore, for an arbitrary acoustic channel, the cross-correlation function of (11) can be modified as:

$$c(t) = IRFFT(H \cdot Y \cdot REF^*) \quad (15)$$

It can be expanded as:

$$c(t) = IRFFT(a_n \omega^n) * IRFFT(Y \cdot REF^*) + IRFFT(a_{n-1} \omega^{n-1}) * IRFFT(Y \cdot REF^*) + \dots + a_0 \cdot IRFFT(Y \cdot REF^*) \quad (16)$$

Where  $IRFFT$  is the inverse real Fourier transform. The inverse Fourier transform of  $\omega^n$  is the  $n_{th}$  derivative of the Dirac delta function which will not generate an output after convolution with the received signal and the reference signal. Therefore, the non-ideal frequency response of the propagation channel will not affect the final cross-correlation output.

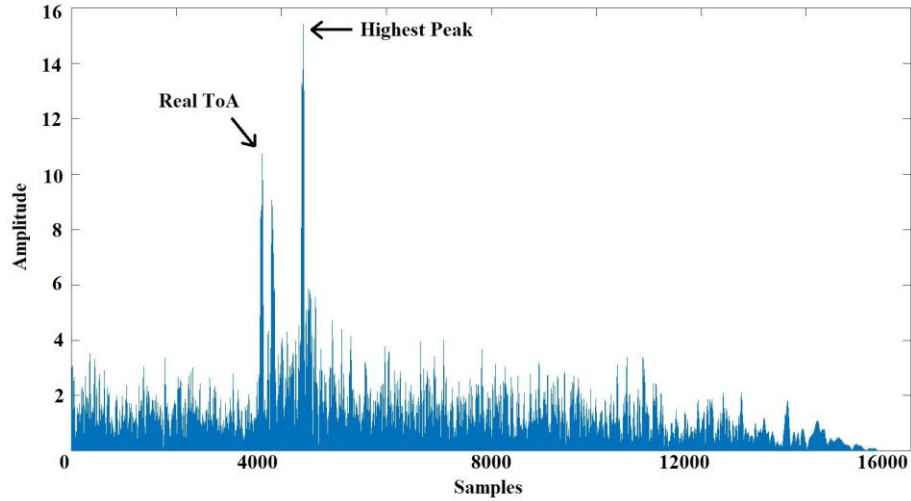


Fig. 6. ToA peak and highest peak.

Due to multipath effects, in some indoor environments, as shown in Fig. 6, the direct path signal's correlation peak is not the highest. Moreover, in some cases the Line-of-Sight (LoS) channel cannot be guaranteed. However, the signal from multi-paths takes longer propagation time compared to the direct path. As a result, we can conclude that in an indoor environment, as long as (a) there exists a direct path between the smartphone speaker and the audio receiver and (b) the SNR is above a certain level, no matter how severe the multipath effects are, the first detectable correlation peak location is always the ToA of the transmitted audio signal. If the LoS condition cannot be guaranteed and the whole received signal only consists of NLoS path signals, the first correlation peak may not represent the ToA. The NLoS case is discussed in the following section.

#### 4.4.3 Noise Filtering

Environmental noise is an important factor in an acoustic channel. There are many high-frequency signals generated by different activities such as the door slamming, high-heeled shoes hitting the ground and tableware collisions. The chirp signal in our system sweeps from 15KHz to 18KHz. A window-based band-pass filter with the passband from 15KHz to 18KHz is implemented to filter out the out-of-band noise. However, there is still in-band noise added to the received signal. Using a matched-filtering approach, the received signal generates outputs only when it matches the reference signal. Pearson correlation coefficient

[24] can be used to measure the similarity between the received and the reference signals. It is defined as:

$$\rho(A, B) = \frac{\text{cov}(A, B)}{\sigma_A \sigma_B} \quad (18)$$

Where  $A$  and  $B$  are the two signals,  $\text{cov}(A, B)$  is the covariance of  $A$  and  $B$ ,  $\sigma_A$  is the standard deviation of  $A$  and  $\sigma_B$  is the standard deviation of  $B$ .

We sampled noise in different indoor environments and computed their Pearson correlation coefficients with a reference signal to estimate the possibilities that they could alter the matched filter's output. A correlation coefficient between -0.1 to +0.1 indicates a negligible correlation [25]. The tests results in Table 1, indicate that in 99.9% cases the correlation coefficients are between -0.1 to +0.1. As a result, it is concluded that the environmental audio noise is unlikely to correlate with a reference chirp signal to alter the matched filter's output.

To further filter out the noise, we used a threshold-based method. We set the threshold according to the average positive amplitude of the cross-correlation output. We first computed this average value and then set the threshold to be four times of the average value. Fig. 7 shows the calculated threshold for the propagation channel. It can be seen that the noise in the cross-correlation output is mainly below the threshold. The solution using a chirp signal with a matched filter presents a good performance in noisy environments.

TABLE I. NOISE CORRELATION COEFFICIENTS TESTS

Scenarios	No or Very Weak Correlation
Shopping Mall	99.97%
Restaurant	99.89%
University Hallway	99.96%
Indoor Parking Lot	99.99%
Noisy Office	99.85%

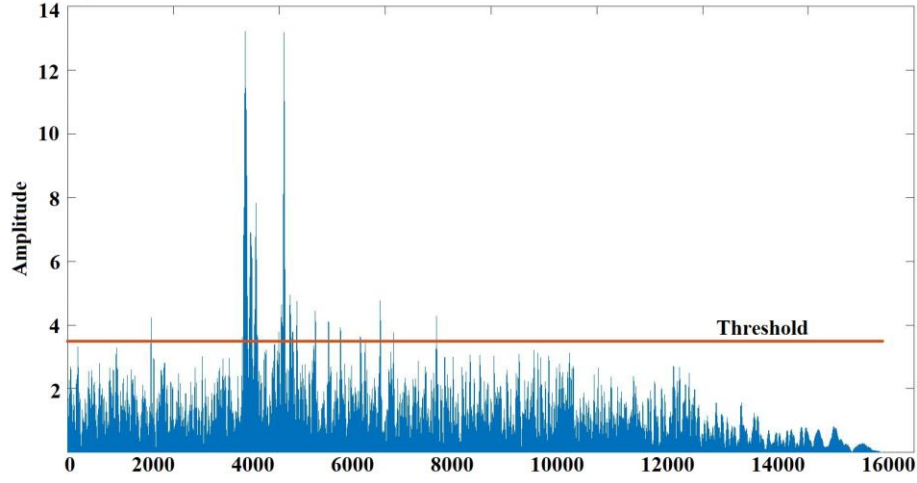


Fig. 7. The calculated threshold for the propagation channel to filter out the noise.

#### 4.4.4 ToA Point Selection

After filtering the noise, in the remaining data blocks all non-zero values are either generated by the matched filter's output or by the noise in the channel. If they are indeed from the matched-filter's output they have to fit in equation (19) which represents the valid output of the matched filter.

$$c[n] = \sqrt{\frac{BN}{F_s}} \cdot \text{sinc} \left[ \pi B \left( \frac{n - N_{ToA}}{F_s} \right) \right] \cdot \cos \left[ 2\pi f_0 \left( \frac{n - N_{ToA}}{F_s} \right) \right] \quad (19)$$

Where  $n$  indicates the sampling points index,  $F_s$  is the sampling rate,  $N$  is the signal's length or the total number of sampling points. For  $N_{ToA} = 6615$ ,  $F_s = 44.1$  KHZ, the positive part of  $c[n]$  is shown in Fig.8. Three features can be extracted from Fig.8, (a) the main lobe of  $c[n]$  has 9 positive audio data point, (b) the two adjunct positive audio data in the main lobe are separated by two or three sampling points from each other and (c) the peak audio data corresponding to the ToA is the local maximum in the main lobe. Therefore, the remaining non-zero values should fit the above-mentioned features if they are generated by the matched filter.

We process the remaining positive audio data by: (a) separating the first audio data block containing the ToA point and (b) discarding the noise after matched-filtering. In the remaining positive data, as shown in Fig. 10 we can have two intuitive observations: (a)

within certain segments there are audio data which are very close to each other to form a cluster, some clusters have more data while others have less, (b) two clusters are separated from each other with a relatively large interval.

As previously demonstrated, since natural environmental noise is not likely to correlate with the reference chirp signal, it will not generate a high amplitude signal at the matched-filtering's output. Since  $c[n]$  in equation (19) has the main lobe with 9 positive audio data, as shown in Fig. 9, a data cluster with more than 9 positive audio data can be considered as a valid data cluster which may contain the ToA point, otherwise they are generated by noise and should be discarded. Moreover, if two blocks of audio data are generated from the target audio signal transmitted through two different paths, due to the propagation time difference, the two blocks of data should be apart from each other with a larger interval compared to the intervals between two neighboring data in the main lobe of  $c[n]$ .

To summarize, a group of audio data with a minimum of 9 positive audio data points can be considered as a valid audio data cluster otherwise it will be discarded. If the two positive audio data points are separated from each other with the interval larger than 3 sampling points, they should be considered as two different clusters. The algorithm initially searches the first positive audio data point, and then it tries to find the next positive one within 3 sampling points' interval. If it can find the next positive one within 3 sampling points' interval, the search for the next positive one will continue. If after 3 sampling points it still can't find a positive value, it considers the last positive audio data as the boundary of the cluster. The total amount of positive audio data is used to determine whether a valid cluster is found or not. Shown in Fig. 10 is the separation of all the positive audio data based on the above procedure. In this way the first cluster can be identified to search for the ToA point, and the remaining noise data will not affect the result as they are discarded.

After separating out the first cluster, we search for the ToA point within the cluster. If the output is indeed the ToA, it should fit  $c[n]$ . In a real scenario, especially in a dense multipath environment, we may get close echoes. In this case, the global maxima may not be the true ToA, but a ToA point is definitely the local maxima according to the third feature of  $c[n]$ . Shown in Fig. 11 is the matched-filter's output in an environment with severe multipath effects. The first local maxima has a lower amplitude compared to the

second and the third local maxima but it corresponds to the real ToA point. We used a sliding window with the size of  $d = 9$  to search for the first local maxima of all positive values, as shown in Fig. 12. The point where the first local maxima locates is the estimated ToA point. In an environment with severe multipath effect, the window size  $d$  can be decreased to distinguish between close echoes.

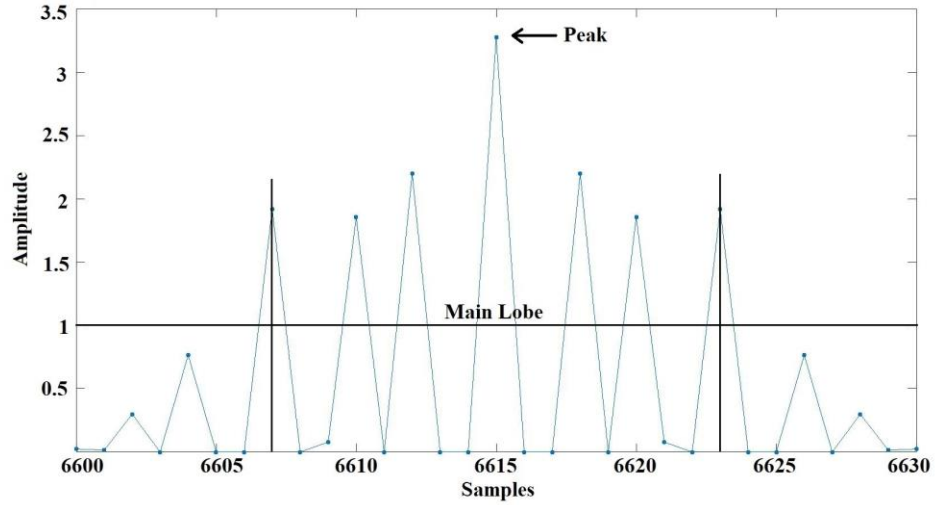


Fig. 8. Positive part of  $c[n]$  with  $N_{ToA} = 6615$ ,  $F_s=44.1$  KHz.

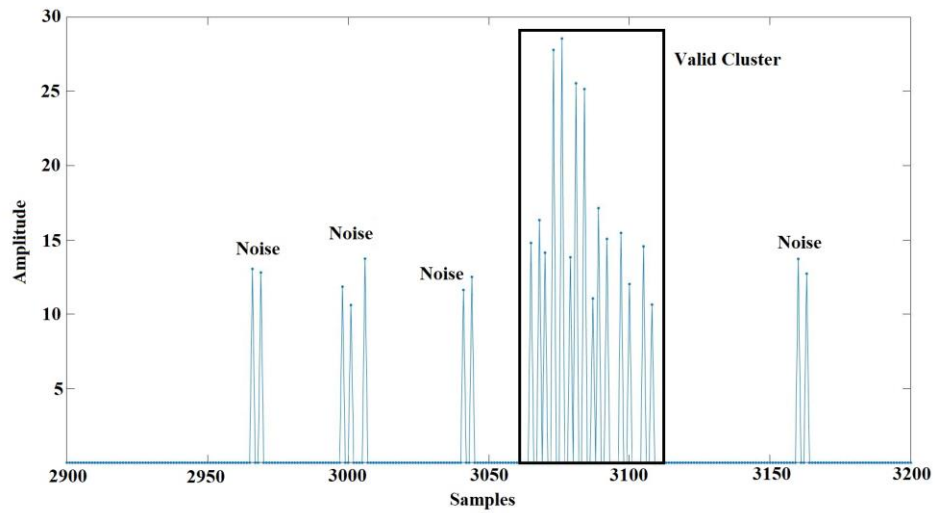


Fig. 9. Valid cluster and noise.

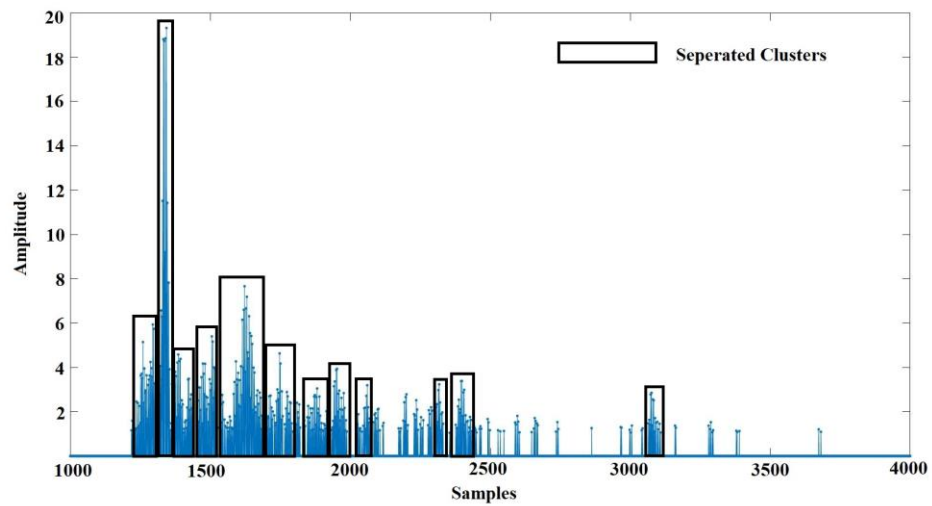


Fig. 10. Separated audio data clusters.

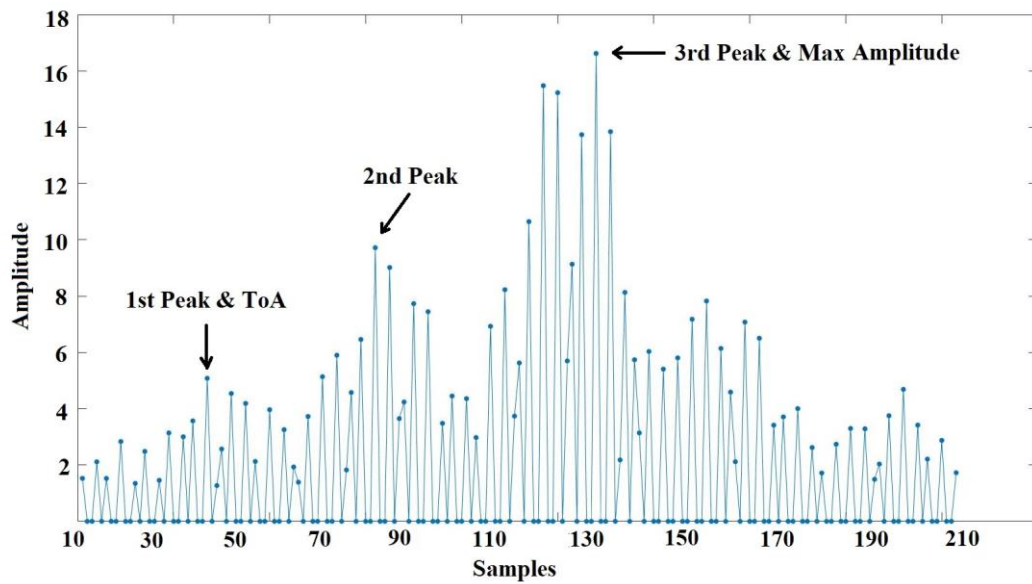


Fig. 11. First local maxima as ToA.

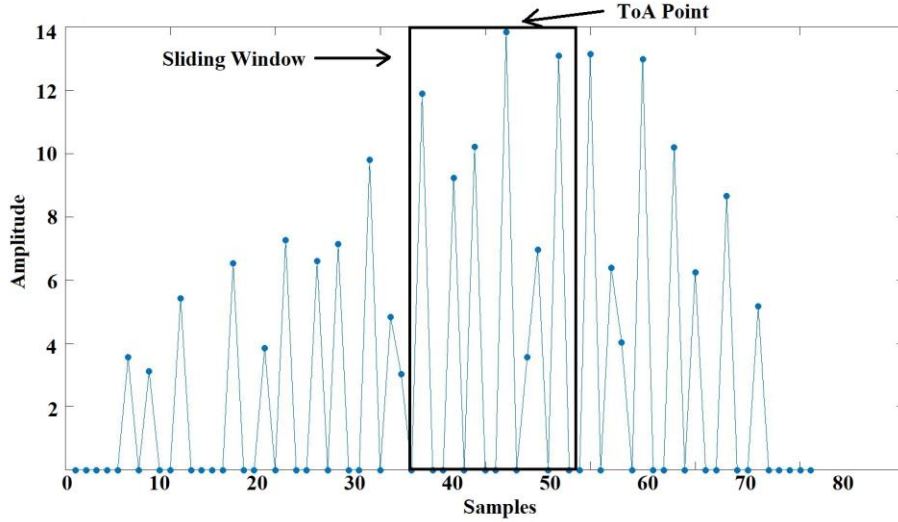


Fig. 12. Local maxima indicating the ToA point.

#### 4.4.5 NLoS Identification

As shown in Fig.13, although there are multipath propagations, there is a direct path channel. Thus, the first detectable cross-correlation peak is the ToA. However, if there is an obstacle between the audio receiver and the smartphone speaker, LoS propagation channel is blocked, as indicated in Fig.14. In this case, the received signal consists the reflected, refracted and diffracted signals. The first local maxima under this circumstance does not represent the ToA. Therefore, we have to identify the NLoS propagation condition and discard the corresponding sampled audio data. When there is no line-of-sight, the number of correlation peaks will increase. Moreover, for a certain transmission distance, the correlation peak amplitude decreases compared to LoS propagation. Fig. 15(a) and Fig. 15(b) show an experiment conducted under the same conditions, except in the first one there was a line-of-sight connection while in the second one there wasn't. We can clearly see that the cross-correlation for the NLoS has more correlation peaks, the output is 'blurred' and the correlation peak amplitudes are lower than the one with the LoS path.

When an audio signal hits an obstacle, the obstacle refracts or reflects the signal generating more correlation peaks at the matched filter's output compared to the LoS condition where the correlation peak is generated by only the direct path signal, as shown in Fig. 14.

Moreover, reflected audio signals experience energy loss which causes the cross-correlation peak amplitude to decrease.

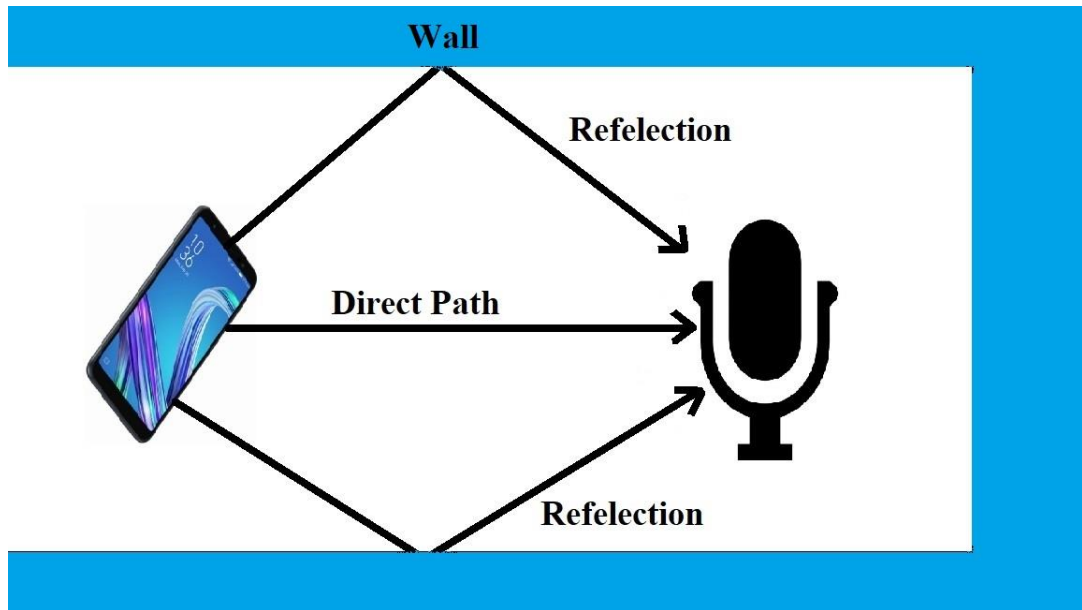


Fig. 13. LoS condition.

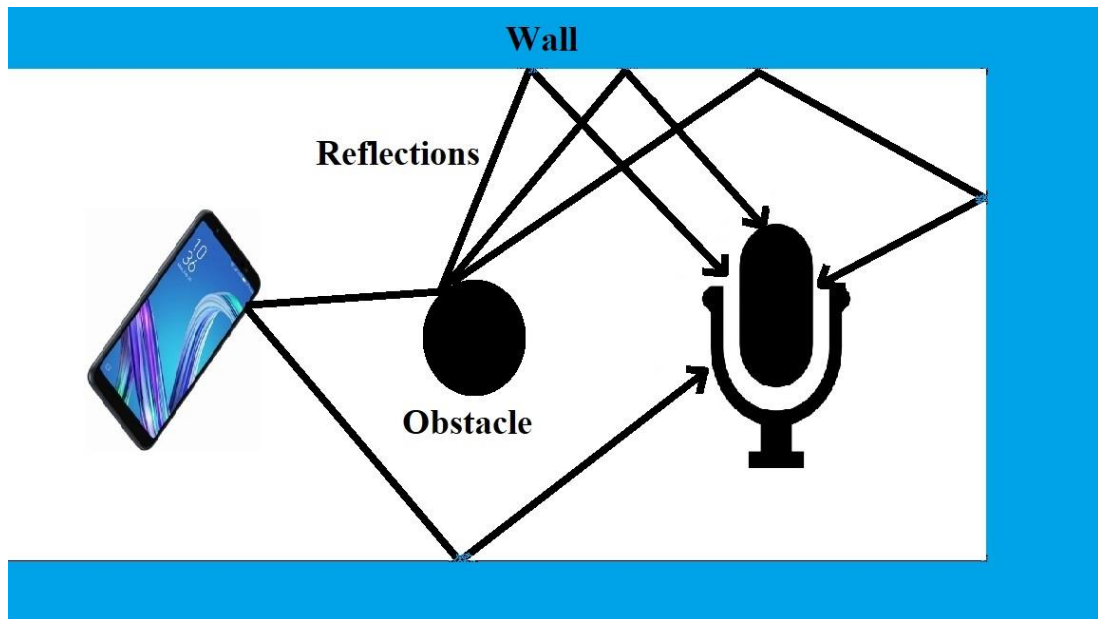
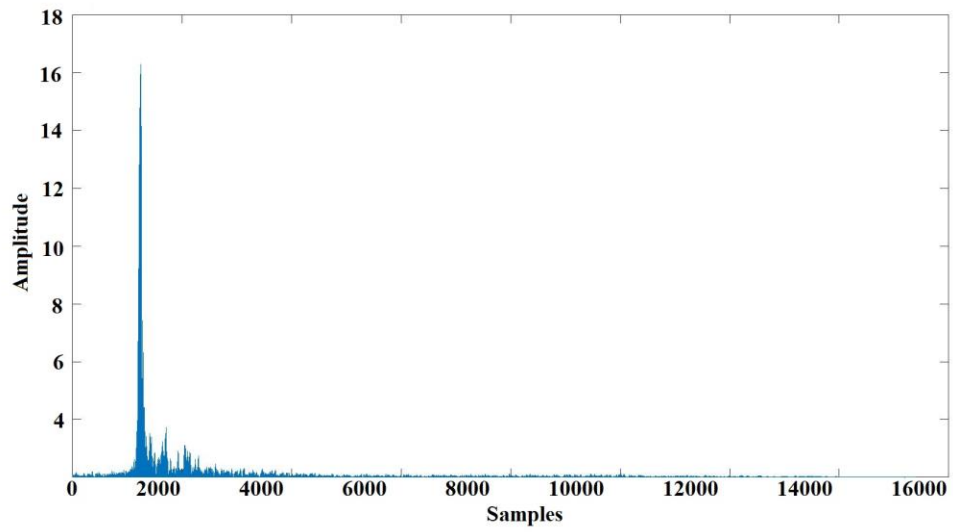
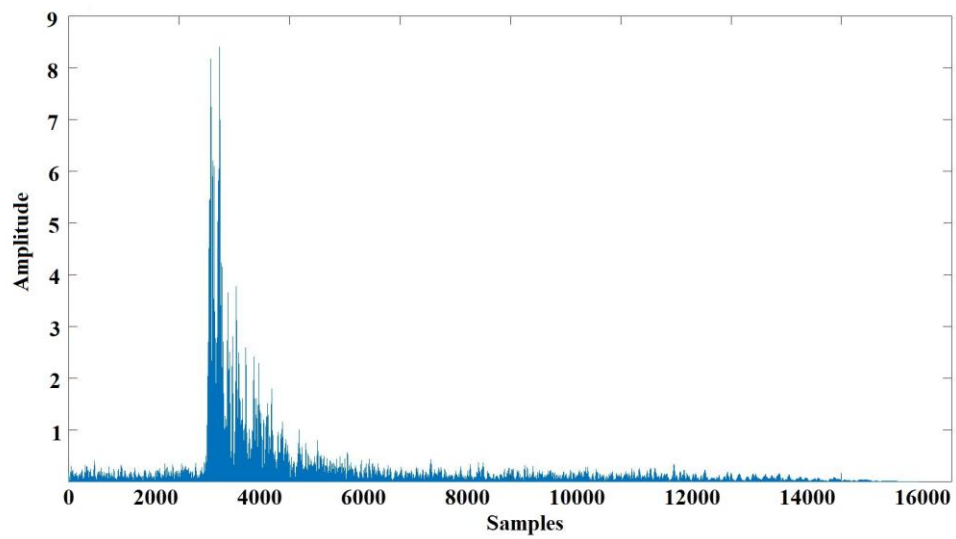


Fig. 14. NLoS condition.



(a)



(b)

Fig. 15. The output of the cross correlation for an experiment where (a) with a line-of-sight connection and (b) without a line-of-sight connection between transmitters and receivers.

In addition to the audio based positioning, the proposed system also supports RSSI based location estimation. The RSSI positioning algorithm is less affected by NLoS propagation, it supports location positioning with a meter-level accuracy. The RSSI based positioning is used as a reference to determine if the position reported in the acoustic mode is valid or not. In the proposed solution, if the differences between the reported position in the acoustic mode and the BLE mode become larger than a threshold  $Th_{dif}$ , the system dumps the result.

## 4.5 Experimental Validation

### 4.5.1 System Prototype

The area of interest is divided into grids where each grid is populated with BLE tags. Each tag consists of SPK0415HM4H microphone, CC1310 sub-1 GHz wireless microcontroller to synchronize audio receivers and CC2640 BLE microcontroller for communication with users. Each tag is also equipped with the required resources to determine the time-of-arrival for transmitted audio signals. A smartphone app is developed using Apache-Cordova platform to test the performance of the implemented positioning system.

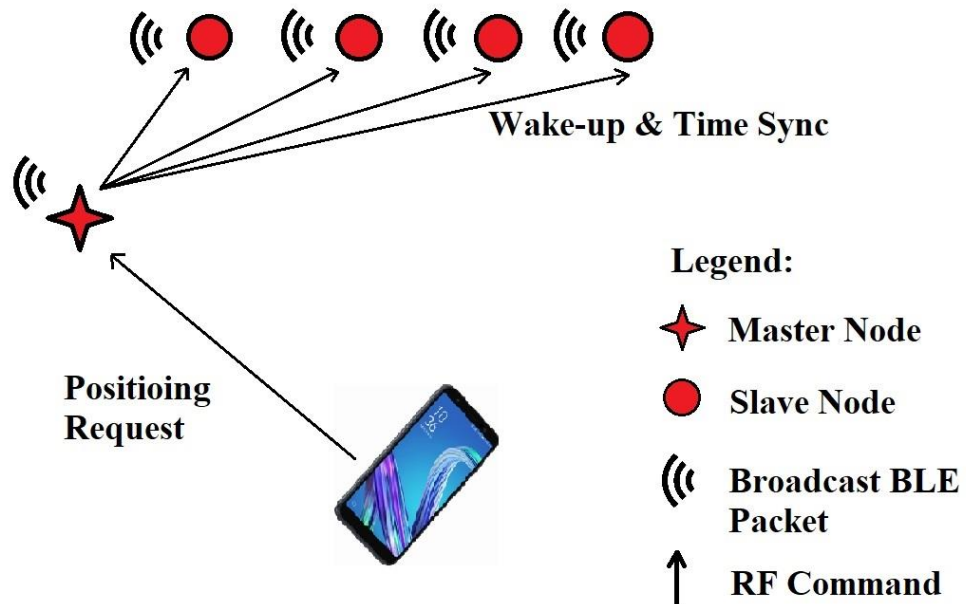


Fig. 16. Wireless communication.

### 4.5.2 Wireless Communication

As shown in Fig.16, an audio receiver in a grid serves as a master BLE access point which receives commands directly from the smartphone. The CC2640 BLE microcontroller at all nodes broadcast BLE packets periodically, these packets can be received by a smartphone to determine its location using the RSSI-based positioning algorithm. These packets also contain audio receiver's ToA estimation results which can be extracted by the developed smartphone app. Once the master node receives the positioning request from a smartphone, it sends a command to the slave nodes in the same grid to wake them up. The slave nodes initially try to synchronize with the master node through sub-1GHz RF. Once they are synchronized, the microphones sample the incoming audio signal to determine the ToAs and estimate the location accordingly. As the system scales, master nodes in different grids may transmit inter-node commands simultaneously, as a result a slave node in a grid may receive several commands at the same time. A grid identifier is used in the inter-node command to allow slave nodes distinguish commands from other grids and discard them. A high-accuracy time synchronization is vital for accurate positioning. The measured time-synchronization error is less than  $30.52\mu\text{s}$  corresponding to a TDoA estimation error of about 1.04 cm. The CC2640 and CC1310 modules are normally in sleep mode, their radio components are only activated for a very short time which reduces the power consumption significantly.

### 4.5.3 Optimal Node Placement

To minimize the TDoA errors, the tags have to be properly positioned in the area. An optimal node placement has a good TDoA error tolerance. A two-dimensional optimal sensor placement for TDoA positioning has been proposed in [26]. To cover a 3D rectangular space in this work, we placed the first 4 nodes at the rectangle's vertexes and positioned the 5th node at the geometric center of the first 4 nodes.

We simulated a rectangular room with the length and the width of 20m, the height of 3m using the above-mentioned node placement strategy. We define the system's TDoA error tolerance ability as:

$$\Delta Error = \frac{|E_x| + |E_y|}{\max(|E_{TDoA}|)} \quad (20)$$

Where  $|E_x|$  and  $|E_y|$  are the absolute errors of the estimated  $x$  and  $y$  coordinates and  $\max(|E_{TDoA}|)$  is the maximum of absolute TDoA estimation error. It's clear that  $\Delta Error$  should be as low as possible to support a good error tolerance ability. During the simulation, each node's  $z$  coordinate changes from  $-25$  cm to  $25$  cm with the step size of  $1$  cm. For each  $z$  coordinates combination, we randomly selected 1000 points in the rectangle area to compute the average of  $\Delta Error$ . We found that as the  $z$  coordinates vary, the average of  $\Delta Error$  shows a periodical change as show in Fig.17. Within a certain segment there are several steps which show similar  $\overline{\Delta Error}$  as local minimums. This result shows that there are several combinations of  $z$  coordinates supporting optimal error tolerance abilities.

#### 4.5.4 Experiment Setup

Since the key parameter in the proposed system is the TDoA estimation. The TDoA estimation experiments were conducted for three scenarios of (a) the smartphone was positioned 20m away from the audio receivers in a quiet environment. (b) The same setup in a noisy environment with an estimated  $-20$  dB SNR and (c) a dense multipath environment where the smartphone was placed 3m far from the audio receivers. The location positioning experiments were conducted in a medium size room with both LoS case and NLoS paths.

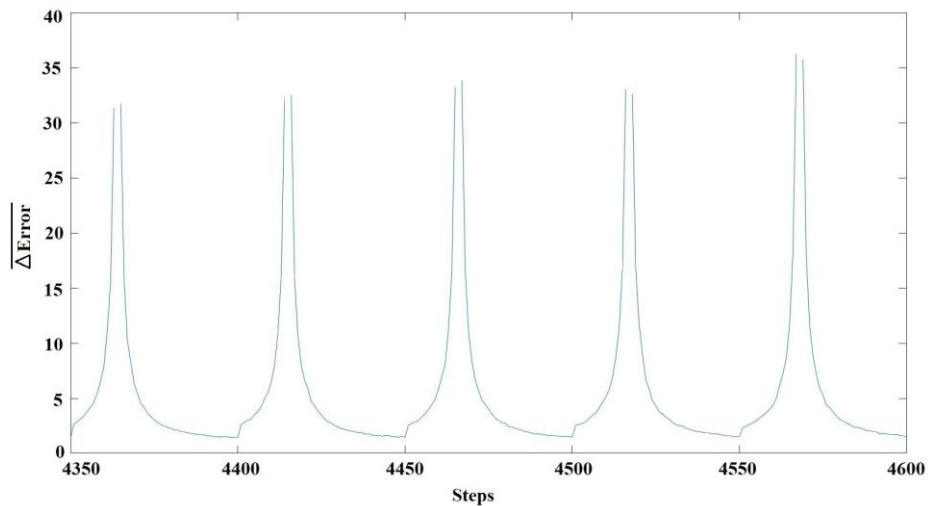


Fig. 17. TDoA error tolerance ability with respect to  $z$  coordinates.



Fig. 18. The area where the experimental measurements were performed.

The first two experiments were conducted in the hallway of CEI building at the University of Windsor, shown in Fig. 18. Audio receivers and smartphone were placed 20m far from each other. For the noisy environment case, an audio player was placed next to the audio receiver tags playing a recording. The estimated SNR was about -20 dB for the transmitted signal. Experiments were also conducted in the CEI building stair entrance. The stair area is small with concrete walls and can be considered an environment with dense multipath effects. In each scenario TDoA measurements were repeated 100 times.

For the location positioning experiment, 4 nodes were placed at the vertexes of a rectangle area with a slight difference in the heights, the 5<sup>th</sup> node was placed at the geometric center of the other 4 nodes. We did experiments at different locations within the rectangle area, 10 times LoS case experiments and 5 times NLoS condition experiments were repeated for each location. Fig. 19, 20 ,21 and 22 show the measurement results.

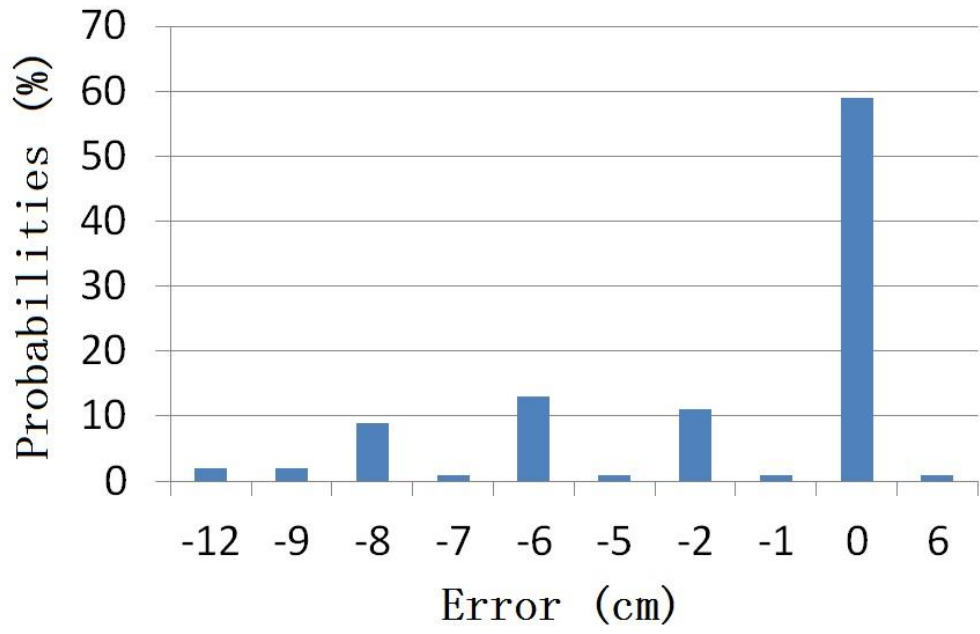


Fig. 19. TDoA experiment results in a quiet environment.

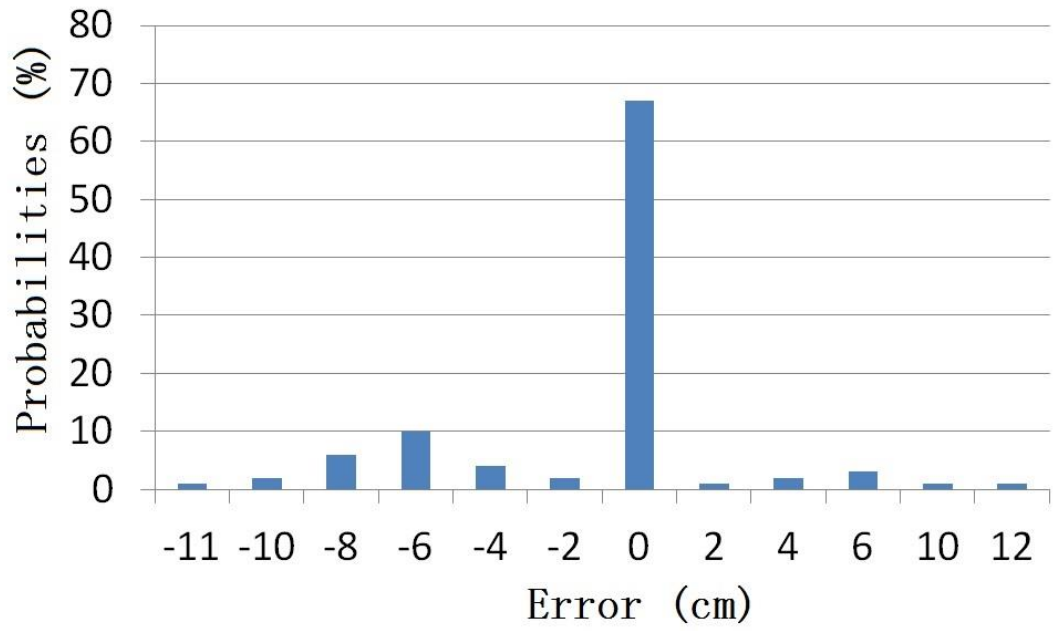


Fig. 20. TDoA experiment results in a noisy environment.

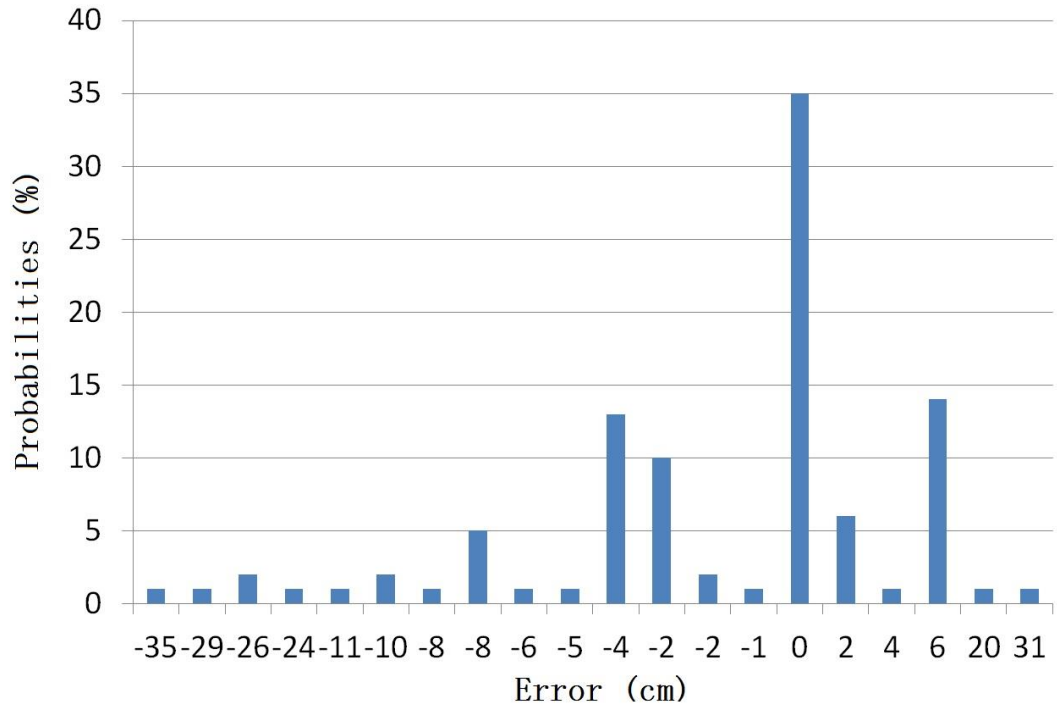


Fig. 21. TDoA results under dense multipath effects.

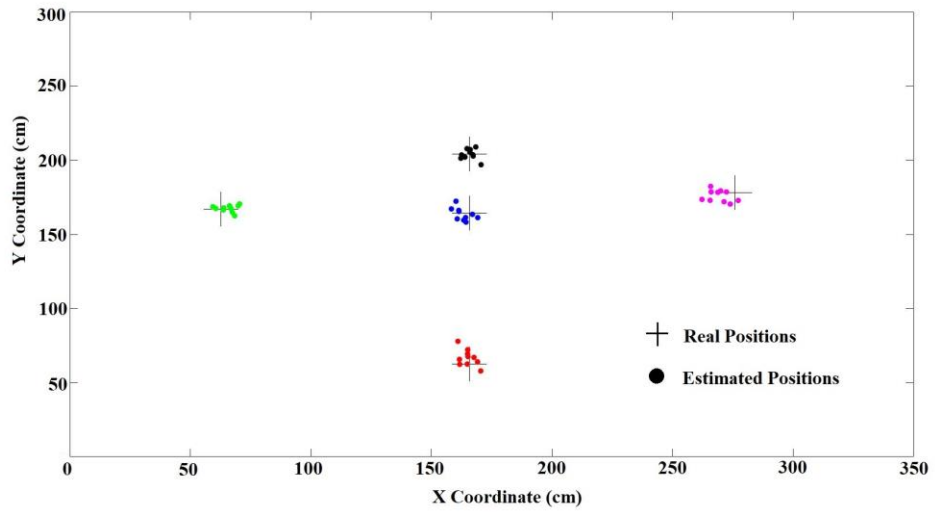


Fig. 22. Position estimation results.

#### **4.5.5 Experiments Results**

For the first experiment, the mean absolute TDoA estimation error was 2.26 cm with the maximum error of 12 cm and the standard deviation of 3.46 cm. In the second experiment, the mean absolute TDoA estimation error was 2.09 cm and the maximum error was 12 cm with the standard deviation of 3.75 cm. In the third experiment, the mean absolute error was 4.53 cm, with the maximum error of 34.5 cm, and the standard deviation of 8.16cm.

As for the location positioning with the LoS path, the estimated x coordinates had the mean absolute error of 3.71 cm, while the error was 2.48 cm for the y coordinate. The x and y coordinates had the max error of 15.40 cm and 15.20 cm respectively. The average of horizontal Euclidean distances error was 5.91 cm and the max error was 16.11 cm.

#### **4.6 Conclusion**

We have proposed a practical indoor positioning solution using RSSI for coarse positioning and near ultrasound audio signal for fine positioning. The proposed solution utilizes BLE nodes for indoor positioning and utilizes cellphones to determine a user location. The proposed solution can operate without internet connectivity since the location is determined by the user's cellphone without the need of a server. To reduce the positioning error and overcome the environmental audio noise, a chirp signal is utilized. A novel digital signal processing algorithm using a matched filter is presented to accurately determine the time-of-arrival for audio signals. The TDoAs are then used for location estimation. RSSI positioning has been used to determine whether a line-of-sight exists for audio based positioning. Experimental measurement results under different conditions indicate that the proposed solution can successfully determine the location of a user with less than 6 cm positioning error on average.

#### **4.7 References**

- [1] S. Pagano, S. Peirani and M. Valle, "Indoor ranging and localisation algorithm based on received signal strength indicator using statistic parameters for wireless sensor networks," *IET Wireless Sensor Systems*, vol. 5, no. 5, pp. 243-249, 10 2015. doi: 10.1049/iet-wss.2014.0027.

- [2] F. Potortì, P. Cassarà and P. Barsocchi, "Device-free indoor localisation with small numbers of anchors," *IET Wireless Sensor Systems*, vol. 8, no. 4, pp. 152-161, 8 2018. doi: 10.1049/iet-wss.2017.0153.
- [3] H. Koyuncu, S. Yang, "Improved adaptive localisation approach for indoor positioning by using environmental thresholds with wireless sensor nodes," *IET Wireless Sensor Systems*, vol. 5, no. 3, pp. 157-165, 6 2015. doi: 10.1049/iet-wss.2013.0100.
- [4] A. Alarifi et al., "Ultra Wideband Indoor Positioning Technologies: Analysis and Recent Advances," *Sensors*, vol. 16, no. 5, p. 707, 2016.
- [5] B. Reynders, S. Pollin, "Chirp spread spectrum as a modulation technique for long range communication," 2016 Symposium on Communications and Vehicular Technologies (SCVT), Mons, 2016, pp. 1-5. doi: 10.1109/SCVT.2016.7797659.
- [6] F. Höflinger et al., "Acoustic Self-calibrating System for Indoor Smartphone Tracking (ASSIST)," 2012 International Conference on Indoor Positioning and Indoor Navigation (IPIN), Sydney, NSW, 2012, pp. 1-9.
- [7] A. Mandal et al., "Beep: 3D indoor positioning using audible sound," Second IEEE Consumer Communications and Networking Conference, 2005. CCNC. 2005, Las Vegas, NV, 2005, pp. 348-353.
- [8] I. Sérgio et al., "Accurate smartphone indoor positioning using a WSN infrastructure and non-invasive audio for TDoA estimation," *Pervasive and Mobile Computing*, Volume 20, 2015, Pages 29-46.
- [9] L. Patrick et al., "ALPS: A Bluetooth and Ultrasound Platform for Mapping and Localization," 73-84. 10.1145/2809695.2809727.
- [10] S. Murata et al., "Accurate Indoor Positioning System using Near-Ultrasonic Sound from a smartphone," Eighth International Conference on Next Generation, Oxford, UK, 2014.
- [11] C. Pérez et al., "Android application for indoor positioning of mobile devices using ultrasonic signals," 2016 International Conference on Indoor Positioning and Indoor Navigation (IPIN), Alcalá de Henares, 2016, pp. 1-7.
- [12] N. Priyantha, A. Chakraborty and H. Balakrishnan, "The cricket location- support system," *Proc. ACM Conference on Mobile Computing and Networking*, 2000.

- [13]A. Ward, A. Jones and A. Hopper, "A New Location Technique for the Active Office," *IEEE Personal Communications*, Vol. 4, No. 5, October 1997, pp. 42-47.
- [14]R. Balani, "Energy Consumption Analysis for Bluetooth, WiFi and Cellular Networks," Document, Electrical Engineering, University of California at Los Angeles.
- [15]L. Zhang et al., "TOA Estimation of Chirp Signal in Dense Multipath Environment for Low-Cost Acoustic Ranging," *IEEE Transactions on Instrumentation and Measurement*. doi: 10.1109/TIM.2018.2844942.
- [16]L. Zhang et al., "Acoustic NLOS identification using acoustic channel characteristics," *Sensors*, 2017, 17 (4) :727 (SCI/EI).
- [17]F. Zaki, R. Rashidzadeh, "An Indoor Location Positioning Algorithm for Portable Devices and Autonomous Machines," *International Conference on Indoor Positioning and Indoor Navigation (IPIN)*, Alcalá de Henares, Spain, 2016.
- [18]"Dev.ti.com. CC13x0 RF User's Guide — CC13x0 Proprietary RF User's Guide 1.01.00 documentation," [online] Available: [http://dev.ti.com/tirex/content/simplelink\\_cc13x0\\_sdk\\_1\\_30\\_00\\_06/docs/proprietary-rf/html/cc13x0/index.html](http://dev.ti.com/tirex/content/simplelink_cc13x0_sdk_1_30_00_06/docs/proprietary-rf/html/cc13x0/index.html) [accessed 17 Dec. 2018].
- [19]P. Stoica, J. Li, "Lecture Notes - Source Localization from Range-Difference Measurements," *IEEE Signal Processing Magazine*, vol. 23, no. 6, pp. 63-66, Nov. 2006.
- [20]C. Mensing, S. Plass, "Positioning Algorithms for Cellular Networks using TDOA," in *Acoustics, Speech and Signal Processing, 2006. ICASSP 2006 Proceedings. 2006 IEEE International Conference*, vol. 4, pp. IV–IV, May 2006.
- [21]X. Jin-yu, W. Wei and Z. Zhong-liang, "A new TDOA location technique based on Taylor series expansion in cellular networks," *Proceedings of the Fourth International Conference on Parallel and Distributed Computing, Applications and Technologies*, Chengdu, China, 2003, pp. 378-381.
- [22]A. Hossain, S. Anower and A. Halder, "A cross-correlation based signal processing approach to determine number and distance of objects in the sea using CHIRP signal," *2015 International Conference on Electrical & Electronic Engineering (ICEEE)*, Rajshahi, 2015, pp. 177-180.

- [23] "Pulse compression", En.wikipedia.org, 2018. [Online]. Available: [https://en.wikipedia.org/wiki/Pulse\\_compression](https://en.wikipedia.org/wiki/Pulse_compression). [accessed 22 Nov. 2018].
- [24] L. Sheugh, H. Alizadeh, "A note on pearson correlation coefficient as a metric of similarity in recommender system," 2015 AI & Robotics (IRANOPEN), Qazvin, 2015, pp.1-6. doi: 10.1109/RIOS.2015.7270736.
- [25] "What does it mean if the correlation coefficient is positive, negative, or zero?", Investopedia, 2018. [Online]. Available: <https://www.investopedia.com/ask/answers/032515/what-does-it-mean-if-correlation-coefficient-positive-negative-or-zero.asp>. [accessed 22 Nov. 2018].
- [26] L. K, S. Hing-Cheung, "A study of two-dimensional sensor placement using time-difference-of-arrival measurements," Digital Signal Processing, vol. 19, no. 4, pp. 650-659, 2009. Available: 10.1016/j.dsp.2009.01.002.

## Chapter -5

### Conclusions and future work

#### 5.1 Conclusions

Design and implementation of an indoor positioning system which supports centimetre level accuracy is a challenging task. In this work an indoor location estimation solution utilizing audio signals is presented to develop a hybrid positioning system with a high level of accuracy. In the proposed solution, cellphones were used to generate high frequency audio signals and Bluetooth Low Energy (BLE) tags were utilized as audio receivers. The location of a cellphone in the environment is determined using the difference time of arrival in the fine positioning mode. The proposed hybrid location positioning system uses the Received Signal Strength (RSS) from BLE nodes for coarse positioning. The BLE RSS positioning mode is also utilized as an auxiliary positioning method to identify the Non-Line-of-Sight (NLoS) propagation in the acoustic mode filter out the outliers.

To address the acoustic interferences in indoor environments and to increase the coverage range, two DSP algorithms were implemented. The first algorithm utilizes a band-pass filter and a moving average filter to determine the time-of-arrival. The second algorithm uses linear frequency modulated chirp signals with a matched-filter to determine the time-of-arrival. The second algorithm can be used in the indoor area with low signal-to-noise ratio and dense multipath effects.

An algorithm is developed to minimize the power consumption by the BLE nodes, each node's RF circuit is only activated at specific time points. Sub-1 GHz RF signals are utilized to achieve a microsecond level time synchronisation between BLE nodes. The smartphones and the positioning system communicate using Bluetooth at the 2.4 GHz band which will not interfere with the inter-node wireless communications.

Experimental results showed the system's positioning accuracy in acoustic mode was high, the average error of location estimations was below 10 cm. The proposed system is also smartphone compatible and low cost, the positioning node's unit price is less than 20 Canadian dollars.

## **5.2 Future Work**

Acoustic TDoA/ToA-based positioning solutions are naturally less robust compared to the BLE or WiFi RSS-based solutions. Moreover, the coverage range in the acoustic mode is limited. The DSP algorithms for dense multipath effects environment and low SNR environment can be improved to increase the system robustness and extend the coverage range while reducing the overall power consumption.

The system's positioning performance under severe Doppler effects should be examined, and the corresponding DSP algorithms should be proposed. Moreover, self-learning algorithms can be developed to overcome the variations in an indoor environment. Finally, an optimization tool can be deployed to fine tune the positioning algorithms to optimize performance parameters of the system.

## APPENDIX : COPY RIGHT PERMISSION



RightsLink®

Home

Create Account

Help



**Title:** A Hybrid Indoor Location Positioning System  
**Conference Proceedings:** 2018 IEEE International Conference on Electro/Information Technology (EIT)  
**Author:** Shuo Li  
**Publisher:** IEEE  
**Date:** May 2018  
Copyright © 2018, IEEE

**LOGIN**  
If you're a [copyright.com](#) user, you can login to RightsLink using your [copyright.com](#) credentials. Already a [RightsLink](#) user or want to [learn more?](#)

### Thesis / Dissertation Reuse

**The IEEE does not require individuals working on a thesis to obtain a formal reuse license, however, you may print out this statement to be used as a permission grant:**

*Requirements to be followed when using any portion (e.g., figure, graph, table, or textual material) of an IEEE copyrighted paper in a thesis:*

- 1) In the case of textual material (e.g., using short quotes or referring to the work within these papers) users must give full credit to the original source (author, paper, publication) followed by the IEEE copyright line © 2011 IEEE.
- 2) In the case of illustrations or tabular material, we require that the copyright line © [Year of original publication] IEEE appear prominently with each reprinted figure and/or table.
- 3) If a substantial portion of the original paper is to be used, and if you are not the senior author, also obtain the senior author's approval.

*Requirements to be followed when using an entire IEEE copyrighted paper in a thesis:*

- 1) The following IEEE copyright/ credit notice should be placed prominently in the references: © [year of original publication] IEEE. Reprinted, with permission, from [author names, paper title, IEEE publication title, and month/year of publication]
- 2) Only the accepted version of an IEEE copyrighted paper can be used when posting the paper or your thesis online.
- 3) In placing the thesis on the author's university website, please display the following message in a prominent place on the website: In reference to IEEE copyrighted material which is used with permission in this thesis, the IEEE does not endorse any of [university/educational entity's name goes here]'s products or services. Internal or personal use of this material is permitted. If interested in reprinting/republishing IEEE copyrighted material for advertising or promotional purposes or for creating new collective works for resale or redistribution, please go to [http://www.ieee.org/publications\\_standards/publications/rights/rights\\_link.htm](http://www.ieee.org/publications_standards/publications/rights/rights_link.htm) to learn how to obtain a License from RightsLink.

If applicable, University Microfilms and/or ProQuest Library, or the Archives of Canada may supply single copies of the dissertation.

## **VITA AUCTORIS**

**NAME:** Shuo Li

**PLACE OF BIRTH:** Nanjing, China

**YEAR OF BIRTH:** 1993

### **Education:**

<b>Master of Applied Science (Electrical and Computer)</b>	December, 2018
University of Windsor	Windsor, ON
<b>Master of Engineering (Electrical and Computer)</b>	December, 2016
University of Windsor	Windsor, ON
<b>Bachelor of Engineering (Electronics and Information)</b>	July, 2015
Southwest Jiaotong University	Emeishan , Sichuan